UNIVERSITY OF BUEA

FACULTY OF SCIENCE DEPARTMENT OF MATHEMATICS

APPLICATION OF THE FINITE ELEMENT METHOD FOR THE COMPUTATION OF THE SOLUTION OF HELMHOLTZ-TYPE BOUNDARY VALUE PROBLEMS IN POLYGONAL DOMAINS

A Thesis submitted to the Department of Mathematics, Faculty of Science, in Partial Fulfilment of the Requirements for the Award of a Master of Science Degree in Mathematics.

By

Wamba Momo Lyse Naomi

SC15P198

B.Sc in Mathematics

Supervised by:

Boniface Nkemzi, PhD

Associate Professor of Mathematics

Head of Department of Mathematics

University of Buea.

September 2017

Dedication

To The Wamba Family.

UNIVERSITY OF BUEA FACULTY OF SCIENCE

CERTIFICATION

This is to certify that the work described in the thesis entitled **Application of the Finite Element Method for the Computation of the Solution of Helmholtz-type Boundary Value Problems in Polygonal Domains** by **Wamba Momo Lyse Naomi** was carried out in the Department of Mathematics under the supervision of

....

Dr. Boniface NKEMZI Date

Acknowledgements

”*Do not be anxious about anything, but in every situation, by prayer and petition, with thanksgiving, present your request to GOD. And the peace of GOD, which transcends all understanding, will guard your hearts and your minds in Christ Jesus.” Philippians 4:6-7.* Only these words express my going through during this research and the love of GOD for which am immensely grateful.

My profound gratitude to my supervisor, Dr. Boniface NKEMZI for his patience, for the useful critiques, valuable and constructive directives I received throughout the work.

My immense gratitude to the entire staff of the Mathematics Department of the University of Buea, to all my lectures for the good training and the moral support they showered me, to my Seniors (PhD students),Mme Mary Fomboh, Mme Stephanie Sonkoue, Mr. Jake Leonard Nkeck and Mr. Ludovic Tchantchou for the useful tips and advices and then to my Classmates.

Big thanks to the African Mathematics Millennium Science Initiative (AMMSI) for the award of the AMMSI-PHILLIP Postgraduate Scholarship-2016 grant that enabled me to carry out my research under the most favourable conditions.

My special thanks to all my family members most especially my most wonderful parents for all their efforts and sacrifices and to my brothers and sisters.

Abstract

The main objective of this thesis is to apply the finite element method to compute the solution of the Helmholtz-type boundary value problems in polygonal domains, see, [19].

As it is well known, the solution of elliptic boundary value problems in general, and Helmholtz-

type equations in particular, in two-dimensional domains with corners may contain singularities, see, [1, 7, 25] and the references cite therein, and these singularities in the solution severely reduce the accuracy of the standard finite element method, see, [12, 16, 32].

In order to achieve the above stated objective, we have developed a software, see, [29], in the Python environment, [26], that applies the P_1- finite element method, see, [27], for the approximation of the solution of the boundary value problem for the Poisson equation and boundary value problems for the Helmholtz-type equations in two-dimensional bounded domains. In order to address the problem of accuracy of the approximation in the case of corner singularities, we have implemented the recently developed predictor corrector adaptive technique due to Nkemzi and Jung, see,[25]. Several numerical experiments are presented to demonstrate the efficiency of our software.

Contents

Notations

Suppose, $u : \mathbb{R}^2 \to \mathbb{R}, x = (x_1, x_2) \in \mathbb{R}^2$.

$\mathbb{R}^2$	2-dimensional space of real numbers
$\mathbb{R}_+$	The space of positive real numbers, that is, $\mathbb{R}_+ = (0, \infty)$
$\mathbb{N}$	The set of natural numbers, that is, {0,1,2,3,...}
$\mathbb{N}^*$	The set of natural numbers excluding zero, that is, {1,2,3,...}
$\emptyset$	The empty set
$Supp$	Support of a function
dim	Dimension
δ_{ij}	Kronecker's symbol. $\delta_{ii} = 1$ and $\delta_{ij} = 0$ for $i \neq j$
α	Multiindex, that is, $\alpha = (\alpha_1, \alpha_2, ..., \alpha_n)$, where $\alpha_i \in \mathbb{N}^*$
$meas(K)$	For $K \subset \mathbb{R}^2$, $meas(K)$ represents the Lebesgue measure (area) of K
u_t	First derivative of the function u with respect to the variable t
u_{tt}	Second derivative of the function u with respect to the variable t
Ω	Bounded domain, that is an open, connected and bounded subset of $\mathbb{R}^2$
$\partial\Omega, \Gamma$	Boundary of Ω
$\overline{\Omega}$	Closure of the domain Ω such that, $\overline{\Omega} = \Omega \cup \Gamma$
$\Gamma_{\mathscr{D}}$	Dirichlet boundary, the solution is specified on this boundary
$\Gamma_{\mathscr{N}}$	Neumann boundary, the derivation of the solution is specified on this boundary

ν	Unit outward normal to the boundary
Δ	Laplace operator, that is, $\Delta u = \sum_{i=1}^{2} u_{x_i x_i}$
div	Divergence operator, that is, $div\mathbf{v}=\frac{\partial v}{\partial x_1} + \frac{\partial v}{\partial x_2}$, where $\mathbf{v}=(v_1, v_2)$
∇	Gradient vector, that is, $\nabla u = (u_{x_1}, u_{x_2})$
γ	Trace operator
A^T	Transpose of the matrix A
det A	Determinant of the matrix A
Σ	Real spectrum of an operator
$C(\Omega)$	Space of continuous functions in Ω
$L^1_{loc}(\Omega)$	Space of locally integrable functions in Ω
$L^1(\Omega)$	The space of Lebesgue measurable and absolutely integrable functions in Ω
$L_2(\Omega)$	The space of all square integrable functions in Ω
$V \subset\subset \Omega$	V is a compact subset of Ω
W^k_p, H^k	Sobolev spaces where $k \in \mathbb{N}, 1 \leq p < +\infty$
$a(.,.)$	Bilinear form.
$f(.)$	Linear form.

Chapter One

Introduction

Most physical phenomena that frequently arise in the mathematical analysis of diverse problems in science (including social sciences) are described and modelled by partial differential equations (PDEs), see for example, [14, 15, 20, 24, 28]. These equations involve an unknown function of two or more variables (which may be a spatial or temporal variable or both) and certain of its partial derivatives, see, [15]. The solutions to these equations are functions as opposed to standard algebraic equations whose solutions are numbers, see, [28]. This work will be concerned with the second-order Helmholtz-type PDEs in polygonal domains. The Helmholtz-type equations fall under a class of second order PDEs called elliptic PDEs which are typical for the description of steady state problems. The motivation for this work arises from the wide application of Helmholtz-type equations and the fact that the domains that appear commonly in nature are of arbitrary shape and usually non-smooth, see for example, [16, 12].

For the Helmholtz-type equations just like for the majority of elliptic PDEs (not to exclude the other classes of second-order PDEs, but to remain focused on the class of interest), finding an exact solution is an expensive task in terms of efforts and there is no certainty on whether this solution found is unique,see, [28]. Thus for these reasons, in most cases, the appropriate way to obtain a solution is by numerical approximation of the equation. With the rapid development and availability of highly perfomant computers, a number of numerical methods have been developed, for example, the finite difference method (FDM),see, [18, 31], the finite volume method (FVM), see, [18], the boundary element method (BEM), see, [23], the finite element method (FEM), see for example, [2, 3, 9, 11, 18, 22, 28, 33], the spectral method, see, [19], etc. As seen in [2], for example, the FEM is the most general and the most efficient tool for the numerical treatment of elliptic PDEs in bounded domains due to the following reasons;

1. **Arbitrary geometries:** The FEM can be applied to domains of arbitrary shape and with any boundary conditions.

2. **Robustness:** In the FEM, the contributions of local approximations over individual elements are assembled together in a systematic way to arrive at a global approximation of a solution to a PDE.

3. **Mathematical foundation:** Due to its success in numerical approximation, the FEM has attracted the attention of mathematicians, physicists, and engineers towards it and thus because of the extensive work done on the mathematical foundations during the seventies and eighties, the FEM now enjoys a rich and solid mathematical basis, like Green's theorem from vector calculus, variational methods from calculus of variations, Sobolev spaces from functional analysis, weak derivatives from differential calculus, etc.

4. **The approximated solution:** The FEM approximates the weak solution to the boundary value problem (BVP) and this solution is always easily obtained at least compared to the classical solution.

The treatment of Helmholtz-type BVPs by the FEM in polygonal domains (that is, domains with straight edges) has appeared to be somewhat problematic, see for example, [1, 5, 25]. That is, the accuracy of the standard FEM near the non-smooth parts of the domain like the corners is significantly abated, due to the singular behaviour of the solution, see,[32]. This singular behaviour of the solution is also observed at points where boundary conditions change. By this singularity, we mean that the required smoothness or regularity of the solution is lost, see, [12, 16]. In [16], for example, it is seen that one may consider the main feature of elliptic BVPs in a domain whose boundary is smooth to be what is called the **shift-theorem**. Phrasing this theorem in the framework of Sobolev spaces (these spaces will be defined in the next chapter) we get that, when the right hand side function in the BVP is given in $W_p^k(\Omega)$, where $1 \leq p < +\infty, k \in \mathbb{N}$, then the corresponding solution u belongs to $W_p^{k+2}(\Omega)$, that is the order of the Sobolev space is moved from k to $k+2$. In this situation, upon approximation of the solution with the FEM, one obtains appropriate convergence rates of the approximated solution, see Theorems 3.5.

Regarding this issue of low accuracy of the FEM on non-smooth domains, the modification of the standard FEM in order to achieve similar results with smooth domains will be considered. In order to do this, we will rely on the literature which says that, with f given in $W_p^k(\Omega)$, the solution u of any linear elliptic BVP in polygonal domains has the following property; there exists numbers c_k such that,

$$u - \sum c_k u_k \in W_p^{k+2}(\Omega)$$

see for example, [12, 16]. In other words, the solution can be decomposed into a well-known singular part that depends on the geometry and the smoothness of the data and a regular part which is as smooth as the right hand side allows, see for example, [5]. In elasticity theory, the unknown coefficients, c_k are referred to as stress intensity factors, see for example, [25] while in mechanics they are called stress intensity distributions, see, [10]. While adapting the FEM, a strategy will also be designed for the computation of these coefficients of singularity. These coefficients describe the strength of the singularity, see, [25]. Several methods have been developed to achieve some or all of the above mentioned objectives; some enable the recovering of the optimal rate of convergence of the FEM without necessarily computing the singularity coefficients like the graded mesh refinement method while others enable the explicit computation of these coefficients of singularity without necessarily having the solution u and finally, other methods exist in which both the singularity coefficients and the solution u can be computed simultaneously like the singular function method, the dual singular function method, the singular complement method, etc, see for example, [25] and the references therein.

The main objectives of this thesis are two fold: (1) Develop a software that applies the P_1- FEM to approximate the solution of the boundary value problem for the Helmholtz-type equations in two dimensional bounded domains constituted of triangles. (2) Adapt the software developed in case there is a singularity in the solution.

This thesis is organized as follows: In Chapter 2, the elliptic BVP is presented and some necessary definitions are given. The weak formulation of the BVP is presented, followed by its well-posedness. Next in Chapter 3, the basic aspects and fundamental concepts of the FEM are discussed together with the convergence scheme. In Chapter 4, the software code developed is presented and for different examples, the convergence rate of the approximate solution are computed. These results are then discussed, followed by some conclusions on the work and any future work is presented.

Chapter Two

Analytical Preliminaries

This chapter is devoted to the boundary value problem for the Helmholtz-type equations. The aim of this chapter is to recall all important aspects that will play a fundamental role through out the work. The chapter is organised as follows; In section 2.1, the classical formulation of the BVP is presented. In section 2.2, some sources of the Helmholtz-type equations are presented. Next, in section 2.3, the variational formulation of the BVP and issues of well-posedness are discussed. Finally in section 2.4 the regularity of the non-smooth solution is discussed.

2.1 The model Boundary Value Problem

Let Ω be an open, connected and bounded subset of $\mathbb{R}^2$. Assume that Ω represents a homogeneous and isotropic material. Given a non-zero function $f \in C(\Omega)$, $g_1 \in C(\Gamma_{\mathscr{D}})$ and $g_2 \in C(\Gamma_{\mathscr{N}})$, consider the following mixed-boundary value problem,

$$\begin{aligned} -\Delta u + \lambda u = f \quad &\text{in} \quad \Omega \subset \mathbb{R}^2, \\ u = g_1 \quad &\text{on} \quad \Gamma_{\mathscr{D}}, \\ \frac{\partial u}{\partial \nu} = g_2 \quad &\text{on} \quad \Gamma_{\mathscr{N}}, \end{aligned} \tag{2.1}$$

where $u \in C^2(\Omega) \cap C^1(\overline{\Omega})$ and λ is a real constant. We assume that the boundary $\Gamma = \overline{\Gamma}_{\mathscr{D}} \cup \overline{\Gamma}_{\mathscr{N}}$ with $\Gamma_{\mathscr{D}} \cap \Gamma_{\mathscr{N}} = \emptyset$ such that, $\frac{\partial g_1}{\partial \nu} = g_2$ on $\overline{\Gamma}_{\mathscr{D}} \cap \overline{\Gamma}_{\mathscr{N}}$ and that $meas(\Gamma_{\mathscr{D}}) > 0$ when $\lambda = 0$. The latter fact will be necessary for the well-posedness of the weak formulation of the BVP (2.1) (this will be defined in Section 2.3). We will impose the condition that our boundary should be Lipschitz so that the unit outer normal vector ν is defined almost everywhere on the boundary.

Definition 2.1. *Suppose $\Omega \subset \mathbb{R}^2$, we say that $\partial\Omega$ is a Lipschitz boundary, if there exists a finite open cover $U^1, ..., U^m$ of $\partial\Omega$ such that for $j = 1, ..., m$.*

- *$\partial\Omega \cap U^j$ is the graph of a Lipschitz function g^j and*
- *$\Omega \cap U^j$ is on one side of this graph.*

The above definition can be found in, [27].

2.1.1 Helmholtz-type equations and the Poisson equation

With regards to the boundary value problem (2.1),it can be observed that the constant $\lambda \in \mathbb{R}$, can take different sets of values within the real line. Due to this, (2.1) can be classified into three different boundary value problems as follows;

1. $\lambda = 0$, gives the **Poisson equation** , see for example, [15],
$$-\Delta u = f. \tag{2.2}$$
2. $\lambda < 0$, that is, $\lambda = -\beta^2, \beta \in \mathbb{R}, \beta \neq 0$, gives the **Helmholtz equation**, see for example, [15],
$$-\Delta u - \beta^2 u = f. \tag{2.3}$$
3. Lastly, $\lambda > 0$, that is, $\lambda = \beta^2, \beta \in \mathbb{R}, \beta \neq 0$, gives the **modified Helmholtz equation**, see for example, [4],
$$-\Delta u + \beta^2 u = f. \tag{2.4}$$

2.1.2 Helmholtz's eigenvalue problem

In mathematics literature, the homogeneous state of (2.3) is referred to as an eigenvalue problem for the Laplace operator $-\Delta$, where β^2 is an eigenvalue, see for example, [15, 19]. Since $f \in C(\Omega)$ is a non-zero function, it may happen that problem (2.3) does not have a unique solution. The following theorems provides the necessary conditions under which a unique solution for (2.3) exists.

Theorem 2.1.

1. *Given $\lambda \in \mathbb{R}$, there exists an at most countable set $\Sigma \subset \mathbb{R}$ such that the BVP (2.1), has a unique weak solution for $f \in C(\Omega)$ if and only if $\lambda \notin \Sigma$*

2. *If Σ is infinite, then $\Sigma = \{\lambda_k\}_{k=1}^{\infty}$, the values of a non decreasing sequence with, $\lambda_k \to \infty$*

The statements and proofs of the above two theorems can be found in [15].

Remark 2.1. *From Theorem 2.1, it follows that;*

1. *Problem (2.1) has a unique weak solution if and only if $\lambda \in \mathbb{R}$ is not an eigenvalue of the operator $-\Delta$.*

2. *As seen in [15], for example, it appears that $\lambda \in \mathbb{R}$ is not an eigenvalue of $-\Delta$ in equation (2.4).*

Thus, subsequently we will assume that, β^2 is not an eigenvalue to ensure the existence of a solution at least in the weak sense for problem (2.3).

2.2 Sources of the Helmholtz-type equations

The elliptic PDEs in Section (2.2.1) appear in a myriad of applications in different areas of mathematical physics, applied mathematics and engineering sciences. Some of these equations are found to appear naturally from general conservation laws of physics such as, the law of conservation of energy for example or can be derived from some of the most important linear PDEs already in existence using sundry methods (separation of variables, Laplace transform, Fourier transform or change of variable), see for example, [15, 19]. This section provides some sources for each Helmholtz-type equation.

2.2.1 The Helmholtz Equation

This equation is also called the reduced wave equation and governs wave propagation in an acoustic medium. The Helmholtz equation can be derived from the heat conduction equation, Schrödinger equation, telegraph and other wave-type or evolutionary equations, see for example, [19]. Subsequently, we show the derivation of the Helmholtz equation from the wave equation by applying the method of separation of variables.

Consider the wave equation

$$\frac{1}{c^2} v_{tt} - \Delta v = 0 \tag{2.5}$$

Where, $t > 0$, $x \in \Omega$, c is a non-zero constant and $v = v(x,t)$ is a real-valued function.We suppose the solution $v(x,t)$ is of the form

$$v(x,t) = T(t)u(x) \quad (x \in \Omega, t > 0);$$

Next, we compute

$$\begin{cases} v_{tt}(x,t) = T''(t)u(x) \\ \\ \Delta v(x,t) = T(t)\Delta u(x) \end{cases} \tag{2.6}$$

Replacing equation (2.6) in (2.5) we get,

$$\frac{1}{c^2}T''(t)u(x) = T(t)\Delta u(x)$$

That is,

$$\frac{1}{c^2}\frac{T''(t)}{T(t)} = \frac{\Delta u(x)}{u(x)} \tag{2.7}$$

for all $x \in \Omega$ and $t > 0$ such that, $T(t), u(x) \neq 0$. We notice that both sides of equation (2.7) depend on different independent variables. Thus for the equation to be valid, both sides must equal a constant (called, the separation constant), say $-\beta^2$. Otherwise, by keeping one independent variable fixed and varying the other will result to one side of the equality changing while the other remains unchanged, thus violating the equality, see for example, [6, 15]. This implies,

$$\frac{1}{c^2}\frac{T''(t)}{T(t)} = -\beta^2 = \frac{\Delta u(x)}{u(x)}$$

Thus, we obtain the Helmholtz eigenvalue problem,

$$-\Delta u(x) - \beta^2 u(x) = 0$$

and the second equation

$$T''(t) + \omega^2 T(t) = 0 \quad \text{where,} \ \ \omega = \beta c$$

The constant ω is called the circular frequency, while β is called the wavenumber and is real whenever ω is real.

Remark 2.2.

The equation $T''(t) + \omega^2 T(t) = 0$ *has solution given by*

$$T(t) = Acos(\omega)t + Bsin(\omega)t$$

for some constants A and B. That is, the solutions are periodic in time. Therefore the time equation T(t) is a harmonic function of the circular frequency ω*, see for example, [19].*

2.2.2 The Modified Helmholtz Equation

This equation is related to steady-state heat conduction governing the heat conduction in fins (surfaces that extend from an object to increase the rate of heat transfer to or from the environment), see for example, [4]. It is known that the modified Helmholtz equation arises whenever there is dimension reduction of the three-dimensional BVP for the Poisson equation into two-dimensions, from the application of the method of separation of variables to the heat equation. Also, (2.4) can be derived from the heat equation as will be shown subsequently, see, [15].

Laplace transform of the Heat Equation

Consider the homogeneous heat equation

$$\begin{aligned} v_t - \Delta v = 0 \quad &\text{in} \quad \Omega \times (0, \infty) \\ v = f \quad &\text{on} \quad \Omega \times \{t = 0\} \end{aligned} \tag{2.8}$$

with non-homogeneous Dirichlet condition. Where $v : \Omega \times [0, \infty) \to \mathbb{R}$ is a function of x and t. The Laplacian is taken with respect to the spatial variables x, and $f : \Omega \times [0, \infty) \to \mathbb{R}$ is given. The heat or diffusion equation describes the evolution in time of the density v of some quantity, such as, heat, chemical concentration, see for example, [15].

We perform the Laplace transform on (2.8) with respect to the time variable. In the beginning, we define the Laplace transform for a function u,see, [15].

Definition 2.2. *If $u \in L^1(\mathbb{R}_+)$, we define its Laplace transform $U(s)$ to be*

$$U(s) := \int_0^\infty e^{-st} u(t) dt \qquad (s \geq 0).$$

Performing the Laplace transform on (2.8), gives;

$$V(x,s) = \int_0^\infty e^{-st} v(x,t) dt \qquad (s > 0)$$

Similarly,

$$\begin{aligned} \Delta V(x,s) &= \int_0^\infty e^{-st} \Delta v(x,t) dt \\ &= \int_0^\infty e^{-st} v_t(x,t) dt \quad \text{since} \quad v_t = \Delta v \quad \text{from equation (2.8)} \end{aligned} \tag{2.9}$$

Now we apply integration by parts to solve the above equation. To this effect, we let;

$$\begin{cases} w = e^{-st} \implies dw = -se^{-st} dt \\ dz = v_t(x,t)\, dt \implies z = v(x,t) \end{cases}$$

Thus, (2.9) becames,

$$\begin{aligned} \int_0^\infty e^{-st} v_t(x,t) dt &= \lim_{R \to \infty} \left(e^{-st} v(x,t) |_0^R \right) + s \int_0^\infty e^{-st} v(x,t) dt \\ &= -v(x,0) + sV(x,s) \end{aligned}$$

Therefore,

$$\Delta V(x,s) = sV(x,s) - f(x), \tag{2.10}$$

since $v = f$ from the boundary condition.

Taking $s > 0$ to be fixed, and $u(x) := V(x, s)$, then (2.10) leads to the modified Helmholtz equation,

$$-\Delta u + \beta^2 u = f \quad \text{in} \quad \Omega,$$

where $s = \beta^2 > 0$.

2.3 Variational Formulation of the BVP

This section is devoted to the variational, also called weak formulation, of the BVP (2.1). The motivation for the transformation of BVP (2.1) from the classical to the variational form is two fold; Firstly, as already mentioned in Chapter 1, it forms the basis of the FEM and secondly, the proof of existence, uniqueness and continuous dependence (on the data) of the solution is achieved in a relatively more comprehensible manner using this form, see for example, [9, 11]. For this weak formulation we will require some simple concepts from linear algebra, which can be found in, [7], notions on Hilbert spaces, and Sobolev spaces.

Definition 2.3. *Let there be given a vector space V, with the norm $\|.\|_V$.*

1. *A mapping $a(.,.) : V \times V \to \mathbb{R}$ is called bilinear if it is linear with respect to the first and second variables. That is, if it satisfies the following condition;*

$$a(\alpha_1 u_1 + \alpha_2 u_2, \beta_1 v_1 + \beta_2 v_2) = \alpha_1\beta_1 a(u_1, v_1) + \alpha_2\beta_1 a(u_2, v_1) + \alpha_1\beta_2 a(u_1, v_2)$$

$$+\alpha_2\beta_2 a(u_2, v_2)$$

for any scalars, $\alpha_1, \alpha_2, \beta_1, \beta_2 \in \mathbb{R}$ and any functions $u_1, u_2, v_1, v_2 \in V$.

2. *A bilinear form;*

   $a(.,.) : V \times V \to \mathbb{R}$ *is said to be continuous if there exists a constant* $M > 0$ *such that;*

$$|a(u,v)| \leq M\|u\|_V\|v\|_V \quad \forall u, v \in V.$$

3. *A bilinear form;*

   $a(.,.) : V \times V \to \mathbb{R}$ *is said to be V-elliptic or coercive if there exists a constant* $\alpha > 0$ *such that,*

$$a(u,u) \geq \alpha\|u\|_V^2 \quad \forall u \in V.$$

4. *A bilinear form;*

   $a(.,.) : V \times V \to \mathbb{R}$ *is said to be symmetric if*

$$a(u,v) = a(v,u) \quad \forall u, v \in V$$

5. *By a linear form;*

   $f : V \to \mathbb{R}$ *we mean a mapping such that,*

$$f(\alpha u + \beta v) = \alpha f(u) + \beta f(v) \quad \textit{for all } u, v \in V \quad \textit{and for all } \alpha, \beta \in \mathbb{R}.$$

6. *A linear form;*

   $f : V \to \mathbb{R}$ *is said to be continuous if there exists a constant* $c > 0$ *such that,*

$$|f(v)| \leq c\|v\|_V \quad \textit{for all} \quad v \in V.$$

Definition 2.4. *Given a complete inner-product space (Hilbert space)*[1] *V, a continuous bilinear form* $a(.,.) : V \times V \to \mathbb{R}$ *and a continuous linear form* $f(.) : V \to \mathbb{R}$*, the abstract*

[1] The following definition is not restricted to Hilbert spaces but to norm linear spaces in general.

problem:

Find $u \in U$ *such that,*

$$a(u, v) = f(v) \quad \textit{for all} \quad v \in V, \tag{2.11}$$

where U *is a closed subset of* V*, is called a variational problem. In case the bilinear form* $a(u, v)$ *in (2.11) is symmetric, the above variational problem is equivalent to another abstract problem called minimisation problem. In the latter, the unknown* u *satisfies;*

$$u \in U \ \textit{ such that } \ J(u) = \inf_{v \in V} J(v)$$

where the set U *is a closed convex subset of* V *and* J *is defined as follows;*

$$J(v) = \frac{1}{2} a(v, v) - f(v)$$

With regards to the minimisation and the variational problems given above, there exists theorems that assert the existence and uniqueness of the solution. In the case of the variational problem (2.11), we have the well-known Lax-Milgram Lemma, whose statement is given below, see, for example [9, 11]. For the proof, the reader is referred to[9, p8] or [11, p32].

Lemma 2.1. *Let* V *be a Hilbert space, let* $a(.,.) : V \times V \to \mathbb{R}$*, a continuous* V*-elliptic bilinear form, and let* $f(.) : V \to \mathbb{R}$*, be a continuous linear form, then problem (2.11) has a unique solution.*

2.3.1 Sobolev spaces

This subsection presents the definition and properties of Sobolev spaces. These spaces will be needed for the variational formulation of problem (2.1), which, based on the literature are the most appropriate spaces for this purpose, see for example, [9]. But before this, we consider another notion of derivatives called weak derivatives. We have the following definitions:

Definition 2.5.

1. *The space,* $C_0^\infty(\Omega)$ *consists of all functions* $v : \Omega \to \mathbb{R}$ *with derivatives of any order having compact support. The support of a function is denoted supp, and defined by;*

$$Supp\ \ v := \overline{\{x \in \Omega,\ \ v(x) \neq 0\}} \subset \Omega$$

see, [9, p 11]. We say that $Supp\, v$ *is compact if it is bounded.*

2. *A vector of the form* $\alpha = (\alpha_1, ..., \alpha_n)$*, where each component* α_i *is a nonnegative integer, is called a multiindex and has order* $|\alpha| = \alpha_1 + ... + \alpha_n$*, see, [15].*

3. $L^1_{loc}(\Omega)$ *is the set of all locally integrable functions. That is, the set of all absolutely integrable functions on every compact subset of their domain of definition. As seen in [15], this is given mathematically by;*

$$L^1_{loc}(\Omega) = \{u : \Omega \to \mathbb{R} | v \in L^1(V) \ \ \textit{for each} \ \ V \subset\subset \Omega\}$$

.

4. *Suppose that* $\alpha \in \mathbb{N}^n$ *is a multi-index. A function* $u \in L^1_{loc}(\Omega)$ *has* $\alpha-$*weak partial derivative denoted* $\partial^\alpha u$*, if,*

$$\int_\Omega u(\partial^\alpha \phi) dx = (-1)^{|\alpha|} \int_\Omega v\phi dx \qquad \forall \phi \in C_0^\infty(\Omega), \tag{2.12}$$

where $v = (\partial^\alpha u) \in L^1_{loc}(\Omega)$*, see for example, [9, p 11].*

The specific Sobolev spaces that will be used throughout are defined below, see, [9, p 11]

Definition 2.6. *For each integer $k \geq 0$, the Sobolev space $H^k(\Omega)$ consist of all those functions $v \in L_2(\Omega)$ for which all weak partial derivatives $\partial^\alpha v$ given in (2.12), with $|\alpha| \leq k$, belong to the space $L_2(\Omega)$. That is,*

$$H^k(\Omega) := \{v \in L_2(\Omega) : \partial^\alpha v \in L_2(\Omega) \ \ \forall \alpha \in \mathbb{N}^n : |\alpha| \leq k\}. \tag{2.13}$$

This space is equipped with:

- **The norm**;

$$\|u\|_{k,\Omega} := \left(\sum_{|\alpha| \leq k} \int_\Omega |\partial^\alpha u|^2 dx \right)^{\frac{1}{2}}. \tag{2.14}$$

- **The semi norm**;

$$|u|_{k,\Omega} := \left(\sum_{|\alpha| = k} \int_\Omega |\partial^\alpha u|^2 dx \right)^{\frac{1}{2}}. \tag{2.15}$$

- **The scalar product**;

$$(u, v)_{k,\Omega} := \sum_{|\alpha| \leq k} (\partial^\alpha u, \partial^\alpha v)_{L_2(\Omega)}. \tag{2.16}$$

Remark 2.3. *The Sobolev space defined in (2.13) is a Hilbert space with respect to the scalar product given in (2.16) .*

Now we give some properties of Sobolev spaces as seen in [9, 27, 31].

1. **Traces, Sobolev spaces on $\partial\Omega$.**

   We assume again that, $\Omega \subset \mathbb{R}^2$ is open and bounded. If $u \in C(\overline{\Omega})$, the boundary values $u|_{\partial\Omega}$ are defined at every $x \in \partial\Omega$.

Theorem 2.2. *Let $\Omega \subset \mathbb{R}^2$ be a bounded domain with smooth or Lipschitz boundary $\partial\Omega$, then there exists a bounded linear operator,*

$$\gamma : H^1(\Omega) \to L_2(\partial\Omega). \tag{2.17}$$

That is, there exists a constant c such that, $\|\gamma(u)\|_{H^0(\partial\Omega)} \leq c\|u\|_{H^1(\Omega)}$, $\forall u \in H^1(\Omega)$. The operator γ is called the trace operator, $\gamma(u)$ is called the trace of u and it is such that, if $u \in C(\overline{\Omega})$, then $\gamma(u) = u|_{\partial\Omega}$

2. **Poincaré inequality**

Theorem 2.3. *Let Ω be bounded. There exists a constant C that depends on Ω such that, for all $v \in H_0^1(\Omega)$*

$$|v|_{0,\Omega} \leq C|v|_{1,\Omega}. \tag{2.18}$$

3. **Green's theorem**

Theorem 2.4. *Let $u, v \in C^1(\overline{\Omega})$, then,*

$$\int_\Omega u_{x_i} v dx = -\int_\Omega u v_{x_i} dx + \int_\Gamma u v \nu_i ds \qquad (i = 1, 2). \tag{2.19}$$

With all the above given, the BVP (2.1) can now be moved, from the classical to the variational form.

Recall the classical formulation of problem (2.1), where $f \in C(\Omega)$, $g_1 \in C(\Gamma_{\mathscr{D}})$, $g_2 \in C(\Gamma_{\mathscr{N}})$ are given functions and $\lambda \in \mathbb{R}$;

$$-\Delta u + \lambda u = f \quad \text{in} \quad \Omega \subset \mathbb{R}^2,$$

$$u = g_1 \quad \text{on} \quad \Gamma_{\mathscr{D}},$$

$$\frac{\partial u}{\partial \nu} = g_2 \quad \text{on} \quad \Gamma_{\mathscr{N}}.$$

- Multiplying the above equation by a test function $v \in C_0^\infty(\Omega)$ and integrating over the entire domain $\Omega \subset \mathbb{R}^2$ gives;

$$
\begin{aligned}
-\Delta uv + \lambda uv &= fv \\
\int_\Omega -\Delta uv dx + \int_\Omega \lambda uv dx &= \int_\Omega fv dx \\
\implies -\int_\Omega \sum_{i=1}^{2} \frac{\partial^2 u}{\partial x_i^2} v dx + \int_\Omega \lambda uv dx &= \int_\Omega fv dx \\
\implies \sum_{i=1}^{2} \int_\Omega -\frac{\partial}{\partial x_i}\left(\frac{\partial u}{\partial x_i}\right) v dx + \int_\Omega \lambda uv dx &= \int_\Omega fv dx
\end{aligned}
$$

- Applying Green's theorem from (2.19), on the above equation gives;

$$\sum_{i=1}^{2} \int_\Omega \frac{\partial u}{\partial x_i}\frac{\partial v}{\partial x_i} dx - \int_{\Gamma_{\mathscr{D}}} \frac{\partial u}{\partial \nu} v ds - \int_{\Gamma_{\mathscr{N}}} \frac{\partial u}{\partial \nu} v ds + \int_\Omega \lambda uv dx = \int_\Omega fv dx$$

Taking the solution space U to be $V_{g_1}(\Omega)$, where;

$$V_{g_1}(\Omega) = \{v \in H^1(\Omega) : v = g_1 \text{ on } \Gamma_{\mathscr{D}}\}, \tag{2.20}$$

and the test space V to be $V_0(\Omega)$, where,

$$V_0(\Omega) = \{v \in H^1(\Omega) : v = 0 \text{ on } \Gamma_{\mathscr{D}}\}. \tag{2.21}$$

Then, the problem;

Find $u \in V_{g_1}(\Omega)$, such that

$$a(u, v) = F(v), \tag{2.22}$$

for all $v \in V_0(\Omega)$, where

$$a(u, v) = \int_\Omega \left(\sum_{i=1}^{2} \frac{\partial u}{\partial x_i}\frac{\partial v}{\partial x_i} + \lambda uv \right) dx, \ \ \lambda \in \mathbb{R} \tag{2.23}$$

$$F(v) = \int_{\Omega} fvdx + \int_{\Gamma_{\mathcal{N}}} g_2 vds. \tag{2.24}$$

The spaces in (2.20) and (2.21) represent the largest possible function spaces for u and v such that all integrals remain finite. Also, all integrals remain finite if we take $f \in L^2(\Omega)$ and $\lambda \in L^\infty(\Omega)$. Now, we check on the solvability of problem (2.22) for the different values of the real scalar λ using the following definition;

2.3.2 Well-posedness

Definition 2.7. *A problem is said to be well-posed according to Jacques Solomon Hadamard see, [28, p5] if;*

i. the solution to the problem exists.

ii. this solution is unique.

iii. this solution depends continuously on the given data.

Lemma 2.2. *Let $\lambda = 0$ in (2.23). Then the problem (2.22) with (2.23) and (2.24) given is well posed.*

Proof.

- The bilinearity of $a(u, v)$ and the linearity of $F(v)$ follow from the linearity of the differential and the integral operators.

- The continuity of the bilinear and the linear forms are done exactly as in Lemma (2.4) below.

- We check on the uniqueness of the solution, which is obtained if the bilinear form is V-elliptic. This will require the well-known Poincaré inequality given in (2.18) above. But as seen in the statement of the inequality, this requires that the solution $u = 0$ on the boundary or on part of the boundary. For this purpose, a function called the Dirichlet lift is used to turn the non-homogeneous Dirichlet condition into a homogeneous one. This process is known as homogenisation and it is achieved through the trace theorem given in (2.17) above.

  Now since Ω is a Lipschitz domain and $g_1 \in H^0(\Gamma_{\mathscr{D}})$, by the trace theorem, g_1 is the trace on $\Gamma_{\mathscr{D}}$ of a non-unique function $\tilde{g}_1 \in H^1(\Omega)$ called the extension of g_1 to Ω (i.e. $\tilde{g}_1 = g_1$ on $\Gamma_{\mathscr{D}}$). Setting,

$$w = u - \tilde{g}_1 \tag{2.25}$$

  and replacing, (2.25) in (2.1) gives the new boundary value problem,

$$\begin{aligned} -\Delta w &= \Delta \tilde{g}_1 + f \quad \text{on } \Omega \\ w &= 0 \qquad\qquad \text{in } \Gamma_{\mathscr{D}} \\ \frac{\partial (w + \tilde{g}_1)}{\partial \nu} &= g_2 \qquad\qquad \text{on } \Gamma_{\mathscr{N}} \end{aligned} \tag{2.26}$$

  Thus, we obtain the new variational problem;

  find $w \in V_0(\Omega)$ such that,

$$a(w, v) = l(v) \quad \text{for all } v \in V_0(\Omega) \tag{2.27}$$

  where,

$$a(w, v) = \sum_{i=1}^{2} \int_{\Omega} \frac{\partial w}{\partial x_i} \frac{\partial v}{\partial x_i} dx \;\; ; \;\; l(v) = \sum_{i=1}^{2} \int_{\Omega} \frac{\partial \tilde{g}_1}{\partial x_i} \frac{\partial v}{\partial x_i} dx + \int_{\Omega} f v dx + \int_{\Gamma_{\mathscr{N}}} g_2 v ds,$$

satisfy the hypotheses of Lax/Milgram lemma with the bilinear form $a(w, v)$ being $V_0(\Omega)$ coercive after employing the Poincaré inequality, that is,

For all $w \in V_0(\Omega)$,

$$a(w, w) = \int_\Omega \{\sum_{i=1}^{2} \left(\frac{\partial w}{\partial x_i}\right)^2\} dx$$

$$\implies a(w, w) = \sum_{i=1}^{2} \int_\Omega \left(\frac{\partial w}{\partial x_i}\right)^2 dx \geq C\|w\|_{1,\Omega}^2 \text{ by (2.18)}$$

therefore, $a(w, w) \geq C\|w\|_{1,\Omega}^2 \ \forall w \in V_0(\Omega)$

Thus, $a(w, w)$ is V-elliptic.

Therefore, problem (2.22) has a unique solution.

- The continuous dependence of the solution on the data, is done in a similar way to that of Lemma (2.4) taking, $\beta = 0$

□

Lemma 2.3. *Let $\lambda = -\beta^2$ then, we have that problem (2.22) with (2.23) and (2.24) given is well posed.*

The structure of the bilinear form with the value of λ given does not permit V-ellipticity of the bilinear form. Thus, Lax/Milgram lemma can not be applied. However, the variational problem is still well-posed but requires some further notions. The proof of lemma 2.3 which can be found in [15, Theorems 5 & 6, p 305-306]

Lemma 2.4. *Let $\lambda = \beta^2$ in (2.23),then problem (2.22) with (2.23) and (2.24) given is well posed.*

Proof.

All that is needed is to verify the hypotheses of the Lax/Milgram given in Lemma (2.1).

- The bilinearity of $a(u,v)$ and the linearity of $F(v)$ follow from the linearity of the differential and the integral operators.

- **Continuity of the bilinear form**

$$
\begin{aligned}
|a(u,v)| &= \left| \int_{\Omega} \left(\sum_{i=1}^{2} \frac{\partial u}{\partial x_i}\frac{\partial v}{\partial x_i} + \beta^2 uv \right) dx \right| \\
&\leq \int_{\Omega} \left| \left(\sum_{i=1}^{2} \frac{\partial u}{\partial x_i}\frac{\partial v}{\partial x_i} + \beta^2 uv \right) \right| dx \\
&\leq \int_{\Omega} \left| \sum_{i=1}^{2} \frac{\partial u}{\partial x_i}\frac{\partial v}{\partial x_i} \right| dx + \int_{\Omega} \left| \beta^2 uv \right| dx \quad \text{by the triangle inequality}
\end{aligned}
$$

$$
\leq \sum_{i=1}^{2} \left(\int_{\Omega} \left| \frac{\partial u}{\partial x_i} \right|^2 dx \right)^{\frac{1}{2}} \sum_{i=1}^{2} \left(\int_{\Omega} \left| \frac{\partial v}{\partial x_i} \right|^2 dx \right)^{\frac{1}{2}}
+ \beta^2 \left(\int_{\Omega} |u|^2 \, dx \right)^{\frac{1}{2}} \left(\int_{\Omega} |v|^2 \, dx \right)^{\frac{1}{2}}
$$

By Cauchy-Schwarz inequality, see,[13, p90]

$$
\leq \sum_{i=1}^{2} |\partial_i u|_{0,\Omega} |\partial_i v|_{0,\Omega} + |\beta^2|_{\infty,\Omega} |u|_{0,\Omega} |v|_{0,\Omega}
$$

$$
\leq \ \max \ \{1, |\beta^2|_{\infty,\Omega}\} \|u\|_{1,\Omega} \|v\|_{1,\Omega}
$$

$$
\therefore |a(u,v)| \leq c \|u\|_{1,\Omega} \|v\|_{1,\Omega} \ \text{ for all } \ u, v \in V
$$

where, $c = \ \max \ \{1, |\beta^2|_{\infty,\Omega}\} \ \geq \ 0$, $\|.\|_{0,\Omega}$ and $\|.\|_{\infty,\Omega}$ denote the norms over $L_2(\Omega)$ and $L_\infty(\Omega)$ respectively for all $\beta \in Ł_\infty(\Omega)$, $\beta^2 \geq 0$ a.e.

- **V-ellipticity of the bilinear form.** The bilinear form $a(u,v)$ is $V_{g_1}(\Omega)$ coercive as shown below;

For all $v \in H_g^1(\Omega)$,

$$
a(v,v) = \int_{\Omega} \{ \sum_{i=1}^{2} \left(\frac{\partial v}{\partial x_i} \right)^2 + \beta^2 v^2 \} dx
$$

$$\geq min\{1,\beta^2\}\int_{\Omega}\Big(\sum_{i=1}^{2}\left(\frac{\partial v}{\partial x_i}\right)^2 dx + \|v\|_{0,\Omega}^2\Big) = min\{1,\beta^2\}\big(|v|_{1,\Omega}^2 + \|v\|_{0,\Omega}^2\big)$$

$$\therefore a(v,v) \geq min\{1,\beta^2\}\|v\|_{1,\Omega}^2$$

$$\therefore a(v,v) \geq \alpha\|v\|_{1,\Omega}^2 \text{ for all } v \in V \tag{2.28}$$

Where $\alpha = min\{1,\beta^2\} > 0$

- **Continuity of the linear form**

$$\begin{aligned}|h(v)| &= \left|\int_{\Omega} fvdx + \int_{\Gamma_2} g_2vds\right| \\ &\leq \int_{\Omega}|fvdx| + \int_{\Gamma_2}|g_2vds| \\ &\leq \int_{\Omega}|fv|\,dx + \int_{\Gamma_2}|g_2v|\,ds\end{aligned}$$

$$\leq \left(\int_{\Omega}|f|^2\,dx\right)^{\frac{1}{2}}\left(\int_{\Omega}|v|^2\,dx\right)^{\frac{1}{2}} + \left(\int_{\Gamma_2}|g_2|^2\,ds\right)^{\frac{1}{2}}\left(\int_{\Omega}|v|^2\,dx\right)^{\frac{1}{2}}$$

$$\leq \|f\|_{0,\Omega}\|v\|_{1,\Omega} + \|g_2\|_{0,\Omega}\|v\|_{1,\Omega}$$

$$\therefore |h(v)| \leq c\|v\|_{1,\Omega} \quad \text{for all } v \in V \quad \text{where} \quad c = \|f\|_{0,\Omega} + \|g_2\|_{0,\Omega} \geq 0$$

- **Continuous dependence of the solution on the data**

The objective here is to establish a linear relationship between the solution u and all the data in the problem (both the source term and the boundary data). Since the value of the solution on the Dirichlet boundary is not taking into account during the variational formulation, we will make use of the process of homogenisation. Thus considering the new variational problem,

$$\begin{aligned}-\Delta w + \beta^2 w &= \Delta\tilde{g}_1 - \beta^2\tilde{g}_1 + f && \text{on } \Omega \\ w &= 0 && \text{in } \Gamma_{\mathscr{D}} \\ \frac{\partial(w+\tilde{g}_1)}{\partial\nu} &= g_2 && \text{on } \Gamma_{\mathscr{N}}\end{aligned} \tag{2.29}$$

which satisfies all hypothesis of Lax/Milgram lemma we have that,

For all $w \in H_0^1(\Omega)$,

$$
\begin{aligned}
\alpha\|w\|_{1,\Omega}^2 &\leq a(w,w) \\
&= h(w) \leq |h(w)| \\
&\leq \|w\|_{1,\Omega}\|\tilde{g}_1\|_{1,\Omega} + \beta^2\|\tilde{g}_1\|_{1,\Omega}\|w\|_{1,\Omega} + \|f\|_{0,\Omega}\|w\|_{1,\Omega} + \|g_2\|_{0,\Omega}\|w\|_{1,\Omega} \\
&\leq \left(\|\tilde{g}_1\|_{1,\Omega} + \beta^2\|\tilde{g}_1\|_{1,\Omega}\| + \|f\|_{0,\Omega} + \|g_2\|_{0,\Omega}\|\right)\|w\|_{1,\Omega} \\
\therefore \|w\|_{1,\Omega} &\leq \lambda\left(\|\tilde{g}_1\|_{1,\Omega} + \beta^2\|\tilde{g}_1\|_{1,\Omega}\| + \|f\|_{0,\Omega} + \|g_2\|_{0,\Omega}\|\right) \quad \text{for all} \quad w \in H_0^1(\Omega)
\end{aligned}
$$

where $\lambda = \frac{1}{\alpha}$, provided $\alpha \neq 0$

□

Lemma 2.5. *The function $\tilde{g}_1$ that extends g_1 to the entire domain is non-unique. That is, the solution u is independent of the choice of $\tilde{g}_1$.*

Proof. In order to proof the Lemma 2.5, we will assume that $\tilde{g}_1$ and $\tilde{g}_2$ are both extensions of g to the entire domain such that, $u_1 = w_1 + \tilde{g}_1 \in H^1(\Omega)$ and $u_2 = w_2 + \tilde{g}_2 \in H^1(\Omega)$ are two weak solutions. We wish to show that, u_1 and u_2 are equal. Now since $u_1 - u_2 \in H_0^1(\Omega)$, by (2.27) the difference $u_1 - u_2 \in H_0^1(\Omega)$ satisfies

$$a(u_1 - u_2, v) = 0 \quad \forall v \in H_0^1(\Omega)$$

Taking, $v = u_1 - u_2$ and using the V-ellipticity of the bilinear form, a in the above equation, we get

$$0 = a(u_1 - u_2, u_1 - u_2) \geq C\|u_1 - u_2\|_{1,\Omega}^2$$

This implies that,

$$\|u_1 - u_2\|_V = 0$$

That is, $u_1 = u_2$ a.e in Ω $\square$

Conclusion: Since the solution space is Hilbert, the bilinear form $a(u, v)$ is continuous and V-elliptic and the linear form $h(v)$ is continuous, the variational problem (2.22) has one and only one solution following Lax/Milgram lemma. And by continuous dependence of the solution on the right hand side, we conclude that the problem (2.22) is **well-posed**. In the next section, we study the structure of the solution of problem (2.10) on a domain with a singular point this brought about by the presence of a corner in the geometry, see, [25].

2.4 Decomposition of the solution of the Helmholtz type equations in a domain with a singular point

Suppose the polygonal domain Ω has only one corner S at the origin in the appropriate local coordinates (r, θ). As defined in [25], we define a small circular sector $\mathcal{K} \subset S$ see Figure 2.1, in the neighbourhood of the corner S with radius R and angle $\omega \in (0, 2\pi]$ by

$$\mathcal{K} := \{(x, y) \in \Omega : x = rsin\theta,\ \ y = rcos\theta, \quad 0 < r < R,\ \ 0 < \theta < \omega\} \qquad (2.30)$$

with boundary $\partial\mathcal{K} = \bar{\Gamma}_0 \cup \bar{\Gamma}_1 \cup \bar{\Gamma}_2$, see Figure 2.1.

Define with respect to S, a smooth cut-off function $\eta \in C^{\infty}[0, \infty)$ by

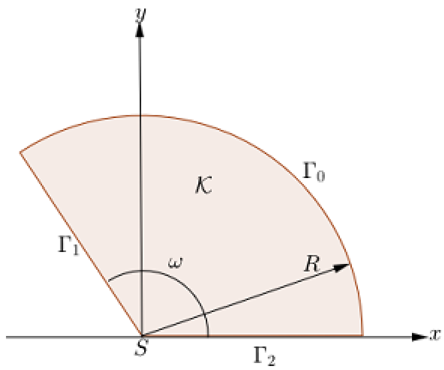

Figure 2.1: The circular sector $\mathcal{K}$

$$\eta(r) := \begin{cases} 1 & \text{for } 0 \le r \le \frac{R}{3} \\ 0 \le \eta \le 1 & \text{for } \frac{R}{3} \le r \le \frac{2R}{3} \\ 0 & \text{for } r \ge \frac{2*R}{3} \end{cases}$$

We use the following notations:

$$\phi_k(\theta) = \begin{cases} \sin(\beta_k\theta) \quad \beta_k = \frac{k\pi}{\omega} & \text{if } \Gamma_1 \cup \Gamma_2 \subset \Gamma_{\mathscr{D}} \\ \cos(\beta_k\theta) \quad \beta_k = ((k-\frac{1}{2})\frac{\pi}{\omega}) & \text{if } \Gamma_1 \subset \Gamma_{\mathscr{D}}, \Gamma_2 \subset \Gamma_{\mathscr{N}} \\ \sin(\beta_k\theta) \quad \beta_k = ((k-\frac{1}{2})\frac{\pi}{\omega}) & \text{if } \Gamma_1 \subset \Gamma_{\mathscr{N}}, \Gamma_2 \subset \Gamma_{\mathscr{D}} \\ \cos(\beta_k\theta) \quad \beta_k = \frac{k\pi}{\omega} & \text{if } \Gamma_1 \cup \Gamma_2 \subset \Gamma_{\mathscr{N}} \end{cases}$$

And have the following result from, [25].

Theorem 2.5. *For $f \in L_2(\Omega)$, let $u \in V_0(\Omega)$ be the weak solution of (2.11). Suppose the domain Ω has only one corner S with angle ω. Then $u \in V_0(\omega)$ can be written in the following form*

$$u = w + \sum_{0<\beta_k<1} \gamma_k s_k(r,\theta) \quad \textit{where } s_k(r,\theta) = r^{\beta_k}\phi_k(\theta)$$

where $w \in H^2(\Omega)$ is a regular part of the solution and the stress intensity factors γ_k

can be computed explicitly using the formula

$$\gamma_k = \frac{1}{\beta_k \omega} \int_{\Omega} f_\eta s_{-k}(r,\theta) dx \tag{2.31}$$

with

$$s_{-k}(r,\theta) = r^{-\beta_k} \phi_k(\theta) \quad \textit{and} \quad f_\eta = \eta(f - \lambda u) - u\Delta\eta - 2\nabla u \cdot \nabla\eta$$

Chapter Three

The Finite Element Method

The FEM originated in aircraft engineering and till present day, still provides the essential tools for approximating solutions of a great variety of problems in engineering and physics. As used today, the FEM represents the confluence of 3 ingredients: Matrix structural analysis, variational approximation theory and digital computing. The aim of this chapter is to understand the theoretical aspects of the FEM in order to develop a FEM software that solves the BVP (2.1). This chapter is organized as follows; In section 3.1, the basic aspects of the FEM are presented. In section 3.2, we give the definition of finite elements as presented in the mathematical literature. Section 3.3, gives an account on how the finite element spaces and the associated linear system are generated. In section 3.4, issues concerning convergence orders of the solution in the $L^2(\Omega)$ and $H^1(\Omega)$ norms are discussed.

3.1 Basic aspects of the FEM.

Below we give some definitions that will be of need throughout. These definitions can be found in [9, 11] for example.

Definition 3.1. *Consider the abstract variational problem given in (2.11) such that the assumptions of Lax-Milgram lemma are satisfied and suppose we have the finite dimensional subspace $V_h \subset V$. Then the associated problem:*

Find $u_h \in V_h$ such that,

$$a(u_h, v_h) = F(v_h), \quad \forall v_h \in V_h \tag{3.1}$$

is called a discrete problem and u_h the discrete solution.

Definition 3.2. *A FEM is said to be conforming when $V_h \subset V$ and when the bilinear and linear forms of the discrete problem are identical to the original ones, see for example, [21].*

In this work, the conforming Galerkin finite element method will be employed. The Galerkin method consists in defining similar problems to the classical problem (2.1) called discrete problems, over finite-dimensional subspaces V_h of the space V, see, [9, 11, 21]. Following Definition (3.2), it follows that the associated Galerkin problem (3.1) is well-posed.

The construction of the subspaces V_h of V is characterized by three basic aspects, see for example, [9, 11, 21]:

♦ Firstly a triangulation or discretization $\mathcal{T}_h$ is established over the set $\bar{\Omega}$, i.e.the set $\bar{\Omega}$ is subdivided into a number of subsets or elements K in such a way that the following conditions are satisfied;

1. The collection of smaller elements K should constitute the entire domain. i.e., $\bar{\Omega} = \cup_{K \in \mathcal{T}_h} K$.
2. For each $K \in \mathcal{T}_h$, the set K is closed and its interior $\mathring{K}$ is non-empty and connected.
3. For two distinct elements $K_1, K_2 \in \mathcal{T}_h$ we have that,$\mathring{K}_1 \cap \mathring{K}_2 = \emptyset$ i.e., elements do not overlap.

Figure 3.1: a) Forbidden triangulation and b) Admissible triangulation

4. For each $K \in \mathcal{T}_h$ any phase of K is either a subset of the boundary $\partial\Omega$ or the phase of any other element $K_1 \in \mathcal{T}_h$.

5. The vertex or node of any element $K \in \mathcal{T}_h$ is either a point on the boundary $\partial\Omega$ or it is a point of another element $K_1 \in \mathcal{T}_h$,see Figure 3.1.

6. For each $K \in \mathcal{T}_h$, the boundary ∂K is Lipschitz-continuous.

7. The triangulations must respect the partition of the boundary and in this case, the Dirichlet and the Neumann boundaries. This to mean that, an edge of an element K, that lies on the boundary Γ cannot be part Dirichlet and part Neumann.

♦ Secondly, the functions $v_h \in V_h$ are piecewise polynomials, that is the space

$$P_K = \{v_h|_K : v_h \in V_h, \ \forall K \in \mathcal{T}_h\}$$

consists of polynomials. In this work, we will deal with polynomials of degree of at most one, these uniquely determined by the values on the vertices of the element K.

♦Thirdly, there should exists a basis in the space V_h whose functions have small supports. That is, in the larger area of Ω the function is zero. This property is essential for numerical purposes since it will produce a sparse matrix, whose storage and solving require less computer memory and fewer arithmetic operations as compared to a dense matrix.

Now we analyse the finite elements obtained after the triangulation of the domain.

3.2 Finite elements

For the construction of the finite dimensional space V_h, the following mathematical definition of the finite element is used, see,[21];

Definition 3.3. *The finite element is a triple* (K, P, Σ)*, where:*

1. *Each element* $K \in \mathcal{T}_h$ *is a closed subset of the entire domain* $\Omega \subset \mathbb{R}^2$ *with a non-empty interior and a Lipschitz boundary.*

2. P *is the space of polynomials of generally real-valued functions defined over each element* $K \in \mathcal{T}_h$*.*

3. Σ *is a finite set of linearly independent forms* $\Phi_i,\ 1 \leq i \leq N$*. These forms are either defined over the space* P *or over a space that contains* P*.*

Definition 3.4. *The set* Σ *is said to be* $P-$ *unisolvent if for any real scalars* $\alpha_i,\ 1 \leq i \leq N$*, there exists a unique function* $p \in P$ *which satisfies;*

$$\Phi_i(p) = \alpha_i, \quad 1 \leq i \leq N$$

Therefore, if Σ *is* P*-unisolvent then there exists functions* $p_i \in P,\ \ 1 \leq i \leq N$*, which satisfy*

$$\Phi_j(p_i) = \delta_{ij}, \quad 1 \leq i \leq N$$

Thus, we can represent each $p \in P$ as

$$p = \sum_{i=1}^{N} \Phi_i(p) p_i$$

where $N = dim\ p$ and $\{p_i\}_{i=1}^{N}$ is a basis of p. The functions $p_i, 1 \leq i \leq N$ are called the basis functions of the finite element and the linear forms $\Phi_i, 1 \leq i \leq N$, are called the degrees of freedom of the element.

Remark 3.1. *In the above notation, h is called the discretization parameter and it is the maximum diameter or length of all elements $K \in \mathcal{T}_h$.*

3.3 Definition of the finite element spaces and generation of the linear system

This section is introduced by giving a brief description of a finite element space generated by Lagrange elements $(K, P_K, \Sigma_K),\ K \in \mathcal{T}_h$. Let $(K_i, P_{K_i}, \Sigma_{K_i})$, $i = 1, 2$ be two adjacent finite elements. Let $S = K_1 \cap K_2$, then for adjacent elements K_1 and K_2,

$$p^1|_S : p^1 \in P_{K_1} = p^2|_S : p^2 \in P_{K_2}$$

We denote the space above P_S. The equality means that, at a vertex common to both K_1 and K_2, the polynomial p^1 defined on K_1 is identical to the polynomial p^2 defined on K_2.

The set $N_i, i = 1, 2, 3$ denotes the number of vertices of each element and, $N_h = \cup_{K \in \mathcal{T}_h} N_i$ denotes the total number of vertices in the entire domain after the triangulation. Then the associated finite dimensional element space V_h is defined as follows;

$$V_h = \{v_h \in C(\overline{\Omega}) \ : \ v_h|_K \in P_K,\ \forall K \in \mathcal{T}_h\}$$

where, P_K is the space of algebraic polynomials of degree ≤ 1. Considering the abstract problem (2.11) and the associated conforming Galerkin problem (3.1),the following theorem turns out to be necessary for solving problem (3.1).

Theorem 3.1. *Solving the discrete problem (3.1) is equivalent to solving the linear system $A\overline{u}_h = \overline{F}_h$, where $A, \overline{u}_h$ and $\overline{F}_h$ are to be defined.*

Proof. Let $\{\phi^i\}_{i=1}^m$ be a basis of the space V_h. We shall look for the discrete solution u_h as a linear combination of the basis functions

$$u_h = \sum_{j=1}^{m} u_j \phi^j$$

Since (3.1) holds for all $v_h \in V_h$, it therefore holds for $v_h = \phi^i, i = 1 : m$. Thus it is true that,

$$\begin{aligned} a\left(\sum_{j=1}^{m} u_j\phi^j, \phi^i\right) &= F(\phi^i) \quad \text{for } i = 1 : m \\ \sum_{j=1}^{m} a\left(\phi^j, \phi^i\right) u_j &= F(\phi^i) \quad \text{for } i = 1 : m \qquad (3.2) \\ A\overline{u}_h &= \overline{F}_h \end{aligned}$$

where $A = (a(\phi^j, \phi^i))_{i,j=1}^m, \qquad \overline{F}_h = (F(\phi^i))_{i=1}^m$ and $\overline{u}_h = (u_1, ..., u_m)$ $\square$

Definition 3.5. *The set $\{\phi\}_{i=1}^m$ is said to be a basis of V_h if;*

- *$\{\phi\}_{i=1}^m$ span or generate V_h*
- *$\{\phi\}_{i=1}^m$ are linearly independent. That is, there exists scalars, $\beta_i, i = 1, ..., m$ such that,*

$$\sum_{i=1}^{m} \beta_i\phi^i = 0 \iff \beta_1 = \beta_2 = ... = \beta_m = 0$$

The matrix A in (3.2) above is called the stiffness matrix and $\overline{F}_h$ the load vector in reference to elasticity theory, see, [21].

Theorem 3.2. *The stiffness matrix A defined in (3.2) is non-singular, symmetric and positive definite.*

Proof. Since the discrete problem satisfies the hypothesis of Lax/Milgram lemma, the bilinearity and V-ellipticity of $a(.,.)$ imply that,

$$\begin{aligned} (A\beta, \beta) &= \sum_{i,j} a(\phi^j, \phi^i)\beta_j\beta_i \\ a\left(\sum_j \beta_j\phi^j, \sum_i \beta_i\phi^i\right) &= a(v_h, v_h) \\ \Longrightarrow\ (A\beta, \beta) &\geq \alpha\|v_h\|^2_{V_h} \ \text{ for all } \ \beta = (\beta_1, ..., \beta_N)^T \in \mathbb{R}^N, \beta \neq 0 \\ \Longrightarrow\ (A\beta, \beta) &> 0 \end{aligned} \tag{3.3}$$

The last inequality holds because $v_h = \sum_i \beta_i\phi^i \neq 0$. Since $v_h \in V_h$, that is, $v_h = \sum_i \beta_i\phi^i$, and $\{\phi^i\}$ is a basis with $\beta \neq 0$. Therefore A is non-singular.

The stiffness matrix is symmetric due to symmetry of the bilinear form $a(.,.)$ and is positive definite as $A(\beta, \beta) > 0$ for all $\beta \neq 0$. $\square$

Let us consider a model problem on which will be computed the stiffness matrix and the load vector. The initial triangulation is given below ,see (Figure 3.2);

Consider the following notations;

N_h	denotes the total number of nodes in $\overline{\Omega}$
R_h	denotes the total number of triangles in $\overline{\Omega}$
K^r	denotes triangle r in $\overline{\Omega}$, that is $r \in \{1, ..., R_h\}$
L	denotes the length of a Neumann edge

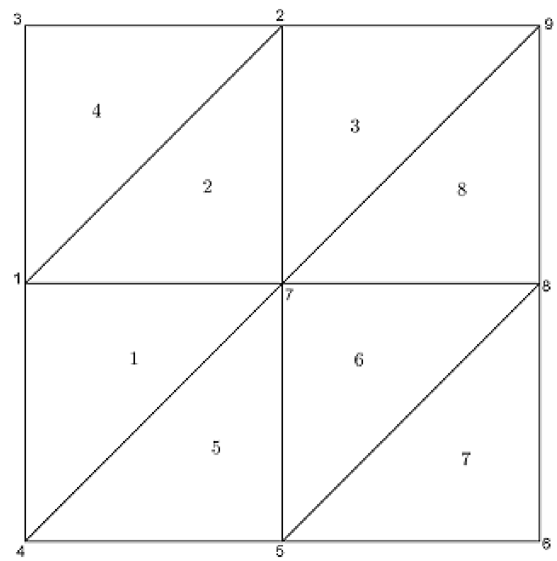

Figure 3.2: Numbering of all triangles and global numbering of nodes.

P^r_α and P^r_β denotes the nodal basis functions evaluated at nodes α and β of triangle r respectively, where $\alpha, \beta \in A^r = \{1, 2, 3\}$

T_L denotes the total number of Neumann edges

We consider the discrete problem (3.1) and have our bilinear form being given by;

$$a(u_h, v_h) = \int_\Omega \left(\frac{\partial u_h}{\partial x}\frac{\partial v_h}{\partial x} + \frac{\partial u_h}{\partial y}\frac{\partial v_h}{\partial y} + \lambda u_h v_h \right)$$

Now if we let,

$$u_h = \sum_{i=1}^{N_h} u_i \phi^i, \quad v_h = \sum_{j=1}^{N_h} v_j \phi^j$$

This implies,

$$\begin{aligned} a(u_h, v_h) &= a\left(\sum_{i=1}^{N_h} u_i\phi^i, \sum_{j=1}^{N_h} v_j\phi^j \right) \\ &= \sum_{r=1}^{R_h} \int_{K^r} \left[\frac{\partial}{\partial x}\left(\sum_{i=1}^{N_h} u_i\phi^i \right) \frac{\partial}{\partial x}\left(\sum_{j=1}^{N_h} v_j\phi^j \right) + \frac{\partial}{\partial y}\left(\sum_{i=1}^{N_h} u_i\phi^i \right) \frac{\partial}{\partial y}\left(\sum_{j=1}^{N_h} v_j\phi^j \right) \right] \\ &\quad dxdy + \left[\lambda \left(\sum_{i=1}^{N_h} u_i\phi^i \right) \left(\sum_{j=1}^{N_h} v_j\phi^j \right) \right] dxdy \end{aligned}$$

$$a(u_h, v_h) = \sum_{r=1}^{R_h} \sum_{i=1}^{N_h} \sum_{j=1}^{N_h} u_i v_j \int_{K^r} \left(\frac{\partial \phi^i}{\partial x} + \frac{\partial \phi^j}{\partial x} + \frac{\partial \phi^i}{\partial y} \frac{\partial \phi^j}{\partial y} + \lambda \phi^i \phi^j \right) dxdy$$

On each triangle, three local nodal basis functions will be defined, but first we denote each of the three vertices of a triangle K^r by;

$$A_1^r, A_2^r, A_3^r$$

and consider the functions ;

$$P_1^r, P_2^r, P_3^r \in P_1$$

such that they satisfy;

$$P_\alpha^r(A_\beta^r) = \delta_{\alpha\beta} \quad \alpha, \beta = 1, 2, 3$$

The entries in the 3×3 matrix for each triangle in the domain Ω are computed using the following;

$$K_{\alpha\beta}^r = \int_{K^r} \left(\frac{\partial P_\alpha^r}{\partial x} \frac{\partial P_\beta^r}{\partial x} + \frac{\partial P_\alpha^r}{\partial y} \frac{\partial P_\beta^r}{\partial y} + \lambda P_\alpha^r P_\beta^r \right) dxdy \quad \alpha, \beta = 1, 2, 3 \tag{3.4}$$

In effect, (3.4) shows that the integrals over Ω have been decomposed as the sum of integrals over the different triangles that constitute the triangulation. To avoid computing this integral R_h times, we use the following reference element;

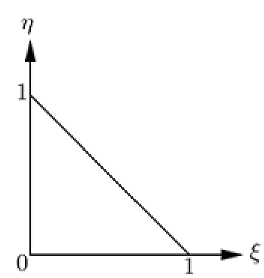

Figure 3.3: Reference triangle $\hat{K}$ with vertices $\hat{A}_1 = (0, 0)$, $\hat{A}_2 = (1, 0)$, $\hat{A}_3 = (0, 1)$.

The local nodal functions in the reference triangle are the three polynomials of degree at most one satisfying;

$$\hat{P}_\alpha(\hat{A}_\beta) = \delta_{\alpha\beta} \quad \alpha, \beta = 1, 2, 3$$

After computation, these functions are explicitly given by,

$$\hat{P}_1 = 1 - \xi - \eta, \quad \hat{P}_2 = \xi, \quad \hat{P}_3 = \eta \tag{3.5}$$

where, (ξ, η) are variables defined over the reference triangle.

Considering the three vertices of a triangle K^r,

$$A_1^r = (x_1, y_1), \;\; A_2^r = (x_2, y_2), \;\; A_3^r = (x_3, y_3)$$

there exists an invertible affine linear map that takes each K^r to $\hat{K}$ such that we have the following transformation;

$$\begin{pmatrix} x \\ y \end{pmatrix} = J_{K^r} \begin{pmatrix} \xi \\ \eta \end{pmatrix} + \begin{pmatrix} x_1 \\ y_1 \end{pmatrix}$$

where,

$$J_{K^r} = \begin{pmatrix} x_2 - x_1 & x_3 - x_1 \\ y_2 - y_1 & y_3 - y_1 \end{pmatrix}$$

is called the Jacobian matrix.

Since, we are dealing with the reference triangle, the integral given in (3.4) has to be transformed into a different coordinate system. Using the chain rule of derivatives, we get the following;

$$\begin{aligned}
\frac{\partial \xi}{\partial x} &= \frac{1}{|J_{K^r}|}(y_3 - y_1) \\
\frac{\partial \xi}{\partial y} &= \frac{1}{|J_{K^r}|}(x_1 - x_3) \\
\frac{\partial \eta}{\partial x} &= \frac{1}{|J_{K^r}|}(y_1 - y_2) \\
\frac{\partial \eta}{\partial y} &= \frac{1}{|J_{K^r}|}(x_2 - x_1)
\end{aligned} \tag{3.6}$$

The integral in (3.4) becomes;

$$\begin{aligned}
K^r_{\alpha\beta} = |J_{K^r}| &\int_{K^r} \left(\frac{\partial \hat{P}_\alpha}{\partial \xi}\frac{\partial \xi}{\partial x} + \frac{\partial \hat{P}_\alpha}{\partial \eta}\frac{\partial \eta}{\partial x} \right) \left(\frac{\partial \hat{P}_\beta}{\partial \xi}\frac{\partial \xi}{\partial x} + \frac{\partial \hat{P}_\beta}{\partial \eta}\frac{\partial \eta}{\partial x} \right) d\xi d\eta \\
+ |J_{K^r}| &\int_{K^r} \left(\frac{\partial \hat{P}_\alpha}{\partial \xi}\frac{\partial \xi}{\partial y} + \frac{\partial \hat{P}_\alpha}{\partial \eta}\frac{\partial \eta}{\partial y} \right) \left(\frac{\partial \hat{P}_\beta}{\partial \xi}\frac{\partial \xi}{\partial y} + \frac{\partial \hat{P}_\beta}{\partial \eta}\frac{\partial \eta}{\partial y} \right) d\xi d\eta \\
+ \lambda |J_{K^r}| &\int_{K^r} \hat{P}_\alpha \hat{P}_\beta \, d\xi d\eta
\end{aligned} \tag{3.7}$$

For each triangle K^r with $r = 1, 2, ..., 8$, in Figure 3.2, we use (3.7) and (3.6) to generate the element stiffness matrix whose coefficients are obtained by computing the following;

$$\begin{aligned}
K^r_{11} &= \frac{1}{2|J_{K^r}|}\left((y_2 - y_3)^2 + (x_3 - x_2)^2\right) + \lambda |J_{K^r}| \int_{K^r} \hat{P}_1 \hat{P}_1 \, d\xi d\eta \\
K^r_{22} &= \frac{1}{2|J_{K^r}|}\left((y_3 - y_1)^2 + (x_1 - x_3)^2\right) + \lambda |J_{K^r}| \int_{K^r} \hat{P}_2 \hat{P}_2 \, d\xi d\eta \\
K^r_{33} &= \frac{1}{2|J_{K^r}|}\left((y_2 - y_1)^2 + (x_2 - x_1)^2\right) + \lambda |J_{K^r}| \int_{K^r} \hat{P}_3 \hat{P}_3 \, d\xi d\eta \\
K^r_{12} &= \frac{1}{2|J_{K^r}|}\left((y_2 - y_3)(y_3 - y_1) + (x_3 - x_2)(x_1 - x_3)\right) + \lambda |J_{K^r}| \int_{K^r} \hat{P}_1 \hat{P}_2 \, d\xi d\eta \\
K^r_{13} &= \frac{1}{2|J_{K^r}|}\left((y_2 - y_3)(y_1 - y_2) + (x_3 - x_2)(x_2 - x_1)\right) + \lambda |J_{K^r}| \int_{K^r} \hat{P}_1 \hat{P}_3 \, d\xi d\eta \\
K^r_{23} &= \frac{1}{2|J_{K^r}|}\left((y_3 - y_1)(y_1 - y_2) + (x_1 - x_3)(x_2 - x_1)\right) + \lambda |J_{K^r}| \int_{K^r} \hat{P}_2 \hat{P}_3 \, d\xi d\eta \\
K^r_{32} &= K^r_{23} \\
K^r_{31} &= K^r_{13} \\
K^r_{21} &= K^r_{12}
\end{aligned} \tag{3.8}$$

The construction of the right hand side of the linear system requires the computation of two vectors

$$\int_{\Omega} fvdx, \quad \int_{\Omega} g_2 vds \tag{3.9}$$

The principle for computing the first integral is that it has to be done just for those nodes that do not belong to the Dirichlet boundary, but in practice, what is done is to compute the integrals for all the boundary nodes and then discard those corresponding to Dirichlet nodes. The element source terms are computed in a similar way to the element stiffness matrix. That is,

$$\begin{aligned}
\int_{\Omega} fv_h dx &= \int_{\Omega} f\left(\sum_{j=1}^{N_h} v_j \phi^j\right) dx \\
&= \sum_{r=1}^{R_h}\sum_{j=1}^{N_h} v_j \int_{K^r} f\phi^j dxdy = \sum_{r=1}^{R_h}\sum_{\beta\in A^r} v_\beta^r \int_{K^r} fP_\beta^r dxdy \\
&= \sum_{r=1}^{R_h} (v_1^r, v_2^r, v_3^r)\,(f_1^r, f_2^r, f_3^r)^T
\end{aligned}$$

where $f_i^r = \int_{K^r} fP_i^r dxdy$, for $i \in \{1, 2, 3\}$

Thus for each triangle in the triangulation, we compute through the reference triangle the 3×1 vector,

$$|J_{K^r}| \int_{K^r} f\hat{P}_\beta^r dxdy, \quad \beta = 1, 2, 3$$

Next, the presence of Neumann boundary conditions imposes the computation of the following integral;

$$\int_{\Gamma_{\mathcal{N}}} g_2 vds = \int_{\Gamma_{\mathcal{N}}} g_2 \left(\sum_{j=1}^{N_h} v_j \phi^j\right) ds$$

The process of computing the above integral is dissimilar to that of computing domain integrals for element stiffness matrices and source terms. First of all the Neumann boundary has to be decomposed into a set of edges that lie on it. This definitely, requires a numbering of the Neumann edges. Thus the above integral becomes:

$$\begin{aligned}\sum_{j=1}^{N_h} v_j \int_{\Gamma_{\mathcal{N}}} g_2 \phi^j ds &= \sum_{T_L} \sum_{j=1}^{N_h} v_j \int_L g_2 \phi^j ds \\ &= \sum_{T_L} \sum_{\beta \in A^r} v_\beta^r \int_L g_2 P_\beta ds, \quad \beta = 1, 2\end{aligned}$$

Let, p_1^L and p_2^L be two vertices of a Neumann edge on the Neumann boundary. Then, there exists an affine mapping that maps element from the reference edge to an arbitrary Neumann edge. If we let this reference edge to be the segment $[0, 1]$, then

$$\phi_1 = 1 - \xi, \quad \phi_2 = \xi$$

are the two basis polynomials of order at most one defined on each node of this reference edge. Thus, the Neumann integrals are computed using the following:

$$\int_{\Gamma_{\mathcal{N}}} g_2 v ds = l \int_0^1 g_2 \hat{P}_\beta \, d\xi, \quad \beta = 1, 2$$

where, l denotes the length of a Neumann edge and is given by;

$$l = \sqrt{(x_1 - x_2)^2 + (y_1 - y_2)^2}$$

In computing the integrals in equation (3.9), we used Gauss-Legendre quadrature. The number of integration points used were such that the error obtained during integration was negligible thus, not affecting the error estimates $\|u - u_h\|$ calculated in Chapter 4.

Assembling the Element Stiffness Matrices and Load Vectors

This aims at forming the system matrix which when solved will yield the approximate value of the solution to the BVP. This system matrix is made up of the global stiffness matrix and the global load vector which in turn are formed by systematically combining entries from the element stiffness matrices and the element load vectors respectively. This process is carried out with the use of a numbering scheme called the global-to-local index. This index, $i(K^r, j)$ relates on each element K^r in the triangulation, the local node number j, to its position i, in the global data structure. A similar process is used to incorporate in the load vector, the Neumann contribution of those boundary nodes located on the Neumann boundary.

Following [8], having our linear system there exists two types of methods for solving them; direct and iterative. According to the theory, direct methods are those that provide an exact solution to the system in a finite number of steps but in practice the solution obtained will be adulterated because errors arise from round off, loss of significant digits,etc. Some of these methods include; Gaussian elimination with backward substitution, the method of inverse, Crammer's rule, LU decomposition, Cholesky factorization, etc. Iterative methods are those convenient for solving sparse matrices. The underlying principle governing an iterative technique for solving linear systems is that, an initial approximation or guess $u^{(0)}$ of the solution is made from which a sequence of vectors $(u^k)_{k=0}^{\infty}$ that converges to u is generated. Some of these iterative methods are; Jacobi's method, Gauss-Seidel method, Conjugate gradient method.

Now, we consider an example, to make the ideas of Section 3.3 more concrete in our minds.

Example 3.1. *In this example, the associated linear system for the Poisson equation* *is generated. We consider the following mixed boundary value problem defined on Ω.*

$$-\Delta u + \lambda u = -\left(2y^2 + 2x^2 - 4\right) + \lambda\left(x^2y^2 - x^2 - y^2 + 1\right) \quad in\ \Omega,$$

$$u = 0 \qquad on\ \Gamma_{\mathscr{D}_1},$$

$$u = 0 \qquad on\ \Gamma_{\mathscr{D}_2},$$

$$\frac{\partial u}{\partial x} = 2y^2 - 2 \qquad on\ \Gamma_{\mathscr{N}_1},$$

$$\frac{\partial u}{\partial y} = 2x^2 - 2 \qquad on\ \Gamma_{\mathscr{N}_2}$$

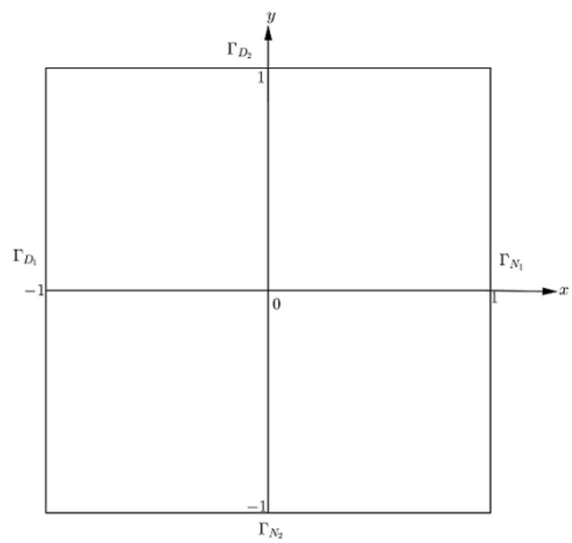

- $\Gamma_{\mathscr{D}_1}, \Gamma_{\mathscr{D}_2}$ - Dirichlet boundaries
- $\Gamma_{\mathscr{N}_1}, \Gamma_{\mathscr{N}_2}$ - Neumann boundaries

Figure 3.4: The domain representing the boundary value problem given above.

The first triangulation of the above domain that will be used for constructing the linear system, is given by Figure (3.2). As mentioned before, the linear system $A\overline{u}_h = \overline{F}_h$ *involves the stiffness matrix A, the vector of unknowns $\overline{u}_h$ and the load vector $\overline{F}_h$. We begin by building the stiffness matrix A.*

1. *We require the values at the vertices of each triangle $K = 1, .., 8$ in the triangulation. Here, these are given by passing the three x-coordinates of each triangle and then the corresponding y-coordinates.*

Triangles=[([-1.0, 0.0, -1.0], [-1.0, 0.0, 0.0]), ([0.0, 0.0, -1.0], [0.0, 1.0, 0.0]), ([0.0, 1.0, 0.0], [0.0, 1.0, 1.0]), ([-1.0, 0.0, -1.0], [0.0, 1.0, 1.0]), ([-1.0, 0.0, 0.0], [-1.0, -1.0, 0.0]), ([0.0, 1.0, 0.0], [-1.0, 0.0, 0.0]), ([0.0, 1.0, 1.0], [-1.0, -1.0, 0.0]), ([0.0, 1.0, 1.0], [0.0, 0.0, 1.0])]

2. *Using the values given above, we calculate the determinant of the Jacobian matrix and the entries of each* 3×3 *element matrices of each triangle. The entries in each element matrix are calculated by evaluating (3.8), where the unknowns in the integrals are given in (3.5). Thus for the example considered above, our element matrices are given as follows;*

$$K^1 = \begin{pmatrix} \frac{1}{2}+\frac{\lambda}{12} & \frac{\lambda}{24} & \frac{-1}{2}+\frac{\lambda}{24} \\ \frac{\lambda}{24} & \frac{1}{2}+\frac{\lambda}{12} & \frac{-1}{2}+\frac{\lambda}{24} \\ \frac{-1}{2}+\frac{\lambda}{24} & \frac{-1}{2}+\frac{\lambda}{24} & 1+\frac{\lambda}{12} \end{pmatrix}, K^2 = \begin{pmatrix} 1+\frac{\lambda}{12} & \frac{-1}{2}+\frac{\lambda}{24} & \frac{-1}{2}+\frac{\lambda}{24} \\ \frac{-1}{2}+\frac{\lambda}{24} & \frac{1}{2}+\frac{\lambda}{12} & \frac{\lambda}{24} \\ \frac{-1}{2}+\frac{\lambda}{24} & \frac{\lambda}{24} & \frac{1}{2}+\frac{\lambda}{12} \end{pmatrix}$$

$$K^3 = \begin{pmatrix} \frac{1}{2}+\frac{\lambda}{12} & \frac{\lambda}{24} & \frac{-1}{2}+\frac{\lambda}{24} \\ \frac{\lambda}{24} & \frac{1}{2}+\frac{\lambda}{12} & \frac{-1}{2}+\frac{\lambda}{24} \\ \frac{-1}{2}+\frac{\lambda}{24} & \frac{-1}{2}+\frac{\lambda}{24} & 1+\frac{\lambda}{12} \end{pmatrix}, K^4 = \begin{pmatrix} \frac{1}{2}+\frac{\lambda}{12} & \frac{\lambda}{24} & \frac{-1}{2}+\frac{\lambda}{24} \\ \frac{\lambda}{24} & \frac{1}{2}+\frac{\lambda}{12} & \frac{-1}{2}+\frac{\lambda}{24} \\ \frac{-1}{2}+\frac{\lambda}{24} & \frac{-1}{2}+\frac{\lambda}{24} & 1+\frac{\lambda}{12} \end{pmatrix}$$

$$K^5 = \begin{pmatrix} \frac{1}{2}+\frac{\lambda}{12} & \frac{-1}{2}+\frac{\lambda}{24} & \frac{\lambda}{24} \\ \frac{-1}{2}+\frac{\lambda}{24} & 1+\frac{\lambda}{12} & \frac{-1}{2}+\frac{\lambda}{24} \\ \frac{\lambda}{24} & \frac{-1}{2}+\frac{\lambda}{24} & \frac{1}{2}+\frac{\lambda}{12} \end{pmatrix}, K^6 = \begin{pmatrix} \frac{1}{2}+\frac{\lambda}{12} & \frac{\lambda}{24} & \frac{-1}{2}+\frac{\lambda}{24} \\ \frac{\lambda}{24} & \frac{1}{2}+\frac{\lambda}{12} & \frac{-1}{2}+\frac{\lambda}{24} \\ \frac{-1}{2}+\frac{\lambda}{24} & \frac{-1}{2}+\frac{\lambda}{24} & 1+\frac{\lambda}{12} \end{pmatrix}$$

$$K^7 = \begin{pmatrix} \frac{1}{2}+\frac{\lambda}{12} & \frac{-1}{2}+\frac{\lambda}{24} & \frac{\lambda}{24} \\ \frac{-1}{2}+\frac{\lambda}{24} & 1+\frac{\lambda}{12} & \frac{-1}{2}+\frac{\lambda}{24} \\ \frac{\lambda}{24} & \frac{-1}{2}+\frac{\lambda}{24} & \frac{1}{2}+\frac{\lambda}{12} \end{pmatrix}, K^8 = \begin{pmatrix} \frac{1}{2}+\frac{\lambda}{12} & \frac{-1}{2}+\frac{\lambda}{24} & \frac{\lambda}{24} \\ \frac{-1}{2}+\frac{\lambda}{24} & 1+\frac{\lambda}{12} & \frac{-1}{2}+\frac{\lambda}{24} \\ \frac{\lambda}{24} & \frac{-1}{2}+\frac{\lambda}{24} & \frac{1}{2}+\frac{\lambda}{12} \end{pmatrix}$$

3. *The next step in the construction of the stiffness matrix is the assembling of elements matrices to form the global matrix. To effectively execute this task, we require the global numbering of each vertex of each triangle as follows;*

   Numbering= [[4, 7, 1], [7, 2, 1], [7, 9, 2], [1, 2, 3], [4, 5, 7], [5, 8, 7], [5, 6, 8], [7, 8, 9]]

   For example,

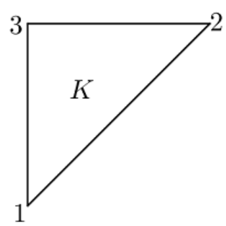

local		global
1	$\longleftrightarrow$	7
2	$\longleftrightarrow$	9
3	$\longleftrightarrow$	2

Figure 3.5: The 3rd triangle and its vertex numbering.

Whenever one is concerned with a certain row/column in the global matrix, we identify where it is found in the set of triangles using the above vector containing the global numberings, collect its position and move to the element stiffness matrices to collect the values which we subsequently add. Thus concerning this example, when $\lambda = 0$, *we obtain the following assembled* 9×9 *matrix;*

$$A = \begin{pmatrix} 2 & 0 & -0.5 & -0.5 & 0 & 0 & -1 & 0 & 0 \\ 0 & 2 & -0.5 & 0 & 0 & 0 & -1 & 0 & -0.5 \\ -0.5 & -0.5 & 1 & 0 & 0 & 0 & 0 & 0 & 0 \\ -0.5 & 0 & 0 & 1 & -0.5 & 0 & 0 & 0 & 0 \\ 0 & 0 & 0 & -0.5 & 2 & -0.5 & -1 & 0 & 0 \\ 0 & 0 & 0 & 0 & -0.5 & 1 & 0 & -0.5 & 0 \\ -1 & -1 & 0 & 0 & -1 & 0 & 4 & -1 & 0 \\ 0 & 0 & 0 & 0 & 0 & -0.5 & -1 & 2 & -0.5 \\ 0 & -0.5 & 0 & 0 & 0 & 0 & 0 & -0.5 & 1 \end{pmatrix}$$

3. *Next is the generation of the load vector. This part involves generating the vector associated to the source term, and that associated to the boundary conditions.*

   [i.] We start by generating the (3×1) *element vectors associated to the source term* f*, following the steps outlined in the theory above, we have when* $\lambda = 0$*;*

$$f^1 = \begin{pmatrix} 0.36664 \\ 0.53333 \\ 0.43335 \end{pmatrix}, f^2 = \begin{pmatrix} 0.6000 \\ 0.53334 \\ 0.5333 \end{pmatrix}, f^3 = \begin{pmatrix} 0.53333 \\ 0.36664 \\ 0.43335 \end{pmatrix}, f^4 = \begin{pmatrix} 0.36664 \\ 0.36667 \\ 0.26666 \end{pmatrix}$$

$$f^5 = \begin{pmatrix} 0.36664 \\ 0.43335 \\ 0.53333 \end{pmatrix}, f^6 = \begin{pmatrix} 0.53333 \\ 0.53332 \\ 0.5999 \end{pmatrix}, f^7 = \begin{pmatrix} 0.36666 \\ 0.26666 \\ 0.36669 \end{pmatrix}, f^8 = \begin{pmatrix} 0.53333 \\ 0.43335 \\ 0.36664 \end{pmatrix}$$

And after assembling this into the global load vector which of course will be *modified later gives us;*

$$f = \begin{pmatrix} 1.33333333 \\ 1.33333333 \\ 0.26666667 \\ 0.73333333 \\ 1.33333333 \\ 0.26666667 \\ 3.33333333 \\ 1.33333333 \\ 0.73333333 \end{pmatrix}$$

[ii.] Next, we do same in order to consider Neumann contributions of the Neumann edges to the load vector. That is, we compute the (1×2) *vectors which we later on assemble into the global load vector using the assembling process described above. Thus, we have for the four different Neumann edges the following contributions;*

$$N^1 = [-0.5, -0.8333333333333334],\ N^2 = [-0.5, -0.8333333333333334]$$

$$N^3 = [-0.8333333333333334, -0.5],\ N^4 = [-0.8333333333333334, -0.5]$$

[iii.] Lastly, we evaluate the solution u *on the Dirichlet nodes, these will be used to correct the load vector once more and reduce both the Stiffness matrix and the load vector.*

Finally we obtain the following Stiffness matrix A *and load vector* $\overline{F}_h$ *whose sizes correspond to the number of non-Dirichlet nodes (both interior nodes and nodes* *that fall on the Neumann boundary).*

$$A = \begin{pmatrix} 2. & -0.5 & -1. & 0. \\ -0.5 & 1. & 0. & -0.5 \\ -1. & 0. & 4. & -1. \\ 0. & -0.5 & -1. & 2. \end{pmatrix}, \quad \overline{F}_h = \begin{pmatrix} -0.33333333 \\ -0.73333333 \\ 3.33333333 \\ -0.33333333 \end{pmatrix}$$

The linear systems generated were solved using Jacobi iteration, Gauss-Seidel and the conjugate gradient as iterative methods and the LU decomposition together with Cholesky factorization as direct methods to obtain the approximate solution u_h for u.

After approximating our solution u, we move on to the approximation of the stress intensity factor defined in (2.31), see, [25].

Theorem 3.3. *(Approximation of the stress intensity factor)*
Suppose the domain Ω has only one corner S. Let $\mathcal{K}$ be a small circular sector in the neighbourhood of S and η a cut-off function defined with respect to S. Let u_h denote the finite element approximation of u. Then the stress intensity factor defined in (2.31) can be approximated by:

$$\gamma_{kh} = \frac{1}{\beta_k \omega} \int_{\mathcal{K}} f_{\eta h} s_k dx \tag{3.10}$$

where $\quad f_{\eta h} := \eta(f - \lambda u_h) - u_h \Delta\eta - 2\nabla u_h \cdot \nabla\eta$

3.4 Error estimates

In this section, the convergence of the error estimates in the $H^1(\Omega)$ and the $L_2(\Omega)$ norms are studied. Initially, suppose that the polygonal domain Ω has no singular point and that we are given the abstract variational problem (2.11) and the associated Galerkin problem (3.1).

Definition 3.6. *Suppose there exists a family of finite element subspaces* $\{V_h\}_{h>0}$ *such that,*

$$\lim_{h\to 0} \|u - u_h\|_V = 0$$

Then we say that the sequence of approximate solutions u_h *obtained after each triangulation converge to the exact solution* u *in the norm* V.

Now, we give the following basic abstract Lemma that provides sufficient conditions for error analysis which can be found in $[9, p104 - 105]$.

Theorem 3.4. ***Céa's Lemma***

There exists, a constant $c > 0$ *independent of the finite element space* V_h *such that,*

$$\|u - u_h\|_V \leq c \inf_{v_h \in V_h} \|u - v_h\| \tag{3.11}$$

Remark 3.2. *Céa's Lemma shows that, the problem of estimating the error* $\|u - u_h\|$ *is reduced to evaluating the distance between the solution* $u \in V$ *and the subspace* $V_h \in V$.

We give the following definition that will be necessary in the next Chapter, see, [9].

Definition 3.7. *Suppose that* u_h *is an approximation of the classical solution* u. *If there exists a constant* $C(u)$ *independent of* h *such that,*

$$\|u - u_h\| \leq C(u)h^\alpha \tag{3.12}$$

holds, then we say that the order of convergence of the solution is α, *where* $\alpha > 0$, *or equivalently, that we have an* $O(h^\alpha)$ *convergence and we simply write*

$$\|u - u_h\| = O(h^\alpha)$$

Now we give the expected convergence rates for the $H^1(\Omega)$ and $L_2(\Omega)$ norms, see, [9, 21].

Theorem 3.5. *Let V be a Hilbert space, $a(.,.) : V \times V \to \mathbb{R}$ a continuous bilinear and coercive form and $f(.) : V \to \mathbb{R}$ a continuous linear form. Let $u \in V$ be the solution of problem (2.1) and $u_h \in V_h$ the solution of problem (3.1), then we have the following error estimates:*

$$\begin{aligned} \|u - u_h\|_{L_2(\Omega)} &= O(h^2) \\ \|u - u_h\|_{H^1(\Omega)} &= O(h) \end{aligned} \tag{3.13}$$

Theorem (3.5) above holds only when the polygonal domain Ω has no point of singularity. The following theorem shall show that, in the presence of a corner, even if our right hand side function f is smooth, the accuracy of the standard finite element is reduced, see, [25] and the references therein.

Theorem 3.6. *Let u be the solution of the boundary value problem (2.1) and u_h its finite element solution defined according to (3.1). Suppose that the domain Ω has only one corner with angle $\omega \geq \pi$. Let γ_k denote the stress intensity factors defined according to (2.31) and γ_{kh} their approximations defined according to (3.10). Then, under the assumption that (3.10) has been accurately computed, the following hold;*

$$\begin{aligned} \|u - u_h\|_{L_2(\Omega)} &= O(h^{2\sigma}) \\ \|u - u_h\|_{H^1(\Omega)} &= O(h^{\sigma}) \\ |\gamma_k - \gamma_{kh}| &= O(h^{2\sigma}) \end{aligned} \tag{3.14}$$

where $0 < \sigma < \frac{\pi}{\omega}$

Given the error estimates in (3.13) and (3.14) above, we describe explicitly how the convergence rate α or σ is calculated. Initially, we assume the value of the discretization parameter h is given by h_i at the i^{th} step and h_{i+1} at the $i+1$ step, where $h_{i+1} = \frac{h_i}{2}$. Assuming the distance between u and u_h at steps i and $i+1$ is bounded following (3.12) where C is assumed to remain constant, we get;

$$\begin{aligned} \|u - u_{h_i}\|_{X(\Omega)} &\leq C(u)h_i^{\alpha} \quad h_i > 0, \\ \|u - u_{h_{i+1}}\|_{X(\Omega)} &\leq C(u)h_{i+1}^{\alpha} \quad h_{i+1} > 0, \end{aligned} \tag{3.15}$$

where, X is either the $H^1(\Omega)$ or $L_2(\Omega)$ norm. Taking the ratio in (3.15) and taking the $\log_2$ we have;

$$\alpha = \log_2 \frac{\|u - u_{h_i}\|_{X(\Omega)}}{\|u - u_{h_{i+1}}\|_{X(\Omega)}} \tag{3.16}$$

(3.16) will be used in Chapter 4 to demonstrate the robustness of the algorithm developed following (3.13). Now we present an alternative way of representing the error estimates. Taking $\log_2$ on both sides of (3.12) we get the following linear relationship between the error estimate $\|u - u_h\|$ and the parameter h;

$$\log_2(\|u - u_h\|_{X(\Omega)}) = \alpha \log_2(h) + \log_2(C) \tag{3.17}$$

(3.17) is a straight line where the rate of convergence α defined in (3.16) is the gradient. Theorem (3.5) gives the optimal rates of convergence of the finite element solution in the $H^1(\Omega)$ and $L_2(\Omega)$ norms. On the other hand, Theorem (3.6), shows that this rate is reduced in both norms when there is a singularity. However the post-processing iterative procedure presented in [25] for computing γ_{kh} and u_h provides a way to improve the accuracy of the approximation such that the optimal rates of convergence are obtained.

Theorem 3.7. *Let u be the weak solution of the boundary value problem (2.1) and let $\tilde{u_h}$ be its finite element approximation. Assume that the domain Ω has only one corner. Let $\tilde{\gamma_{kh}}$ be the approximations of the stress intensity factors γ_k from (2.31). Then one has the following;*

$$\|u - \tilde{u}_h\|_{H_l} = O(h^{2-l}) \;\; l = 0, 1$$

$$|\gamma_k - \tilde{\gamma}_{kh}| = O(h^2)$$

where, $\tilde{u}_h, \tilde{\gamma}_{kh}$ are defined as in the post processing iterative procedure in [25].

Theorem (3.7) can be found in [25]

Chapter Four

Numerical Experiments

The aim of this chapter is to provide for domains, with and without point of singularities, the convergence orders of the solution of the Poisson equation and Helmholtz-type equations, both in the $L_2(\Omega)$ and $H^1(\Omega)$ norms. The major tool for this chapter is a software program developed in the PYTHON environment, [29]. This chapter is organised as follows; In section 4.1, a description of the programming language used and the software developed will be given. Section 4.2 presents convergence orders, α for different concrete problems after analysis with the software. Finally in section 4.3, conclusions on the work and futures perspectives are discussed.

4.1 Description of the Software developed

As an overview we have that, given a domain formed by a collection of triangles of any shape and on which Dirichlet and Neumann boundary conditions are specified, both the Poisson equation and Helmholtz-type equations are solved. The domain is refined for a number of times specified by the user and on each refinement, the stiffness matrix and the load vector are built, solved and error estimates are calculated. In case the domain has a point of singularity, the adaptation is also carried out using the algorithm described in [25]. The software developed is constituted of independent sub-modules with each taking specific inputs, producing outputs, while playing a specific and well-defined function as described below, see, [29].

InputPoly- This function is used to enter the polygonal domain Ω and this is done through an external file that is imported into the PYTHON code and returns a plot of the entire domain.

AllEdges- This function is used to collect all edges in the domain with the boundary function defined on each.

BEdges- This function separates the edges in the original domain as either Dirichlet or Neumann edges.

Ref- This functions refines the domain for a number of times requested by the user. This sub-module returns a vector containing all coordinates of triangles after refinement.

Plotting- This function plots the domain after refinement on an appropriate coordinate axis and saves a copy of the plot in the machine.

Node- This functions is used to collect all nodes coordinates in the domain and global numbering of nodes.

Boundary- This function is used to classify the nodes on the boundary as either Dirichlet or Neumann nodes. This function is particularly useful when considering Dirichlet Boundaries and correcting the right hand side.

NeumannE- This function serves for the creation of Neumann edges after refinement. This will be useful to calculate the Neumann contribution of each node on a Neumann edge.

NNumbre- The purpose of this function is to collect all triangles in the domain using the global numbering of their nodes. This function is of foremost importance during assembling.

Matrix- Here we build the element stiffness matrices and simultaneously assemble them into the global stiffness matrix A, which is returned as the output here.

Load- This function calculates the element load vectors and simultaneously assembles then into the global load vector.

Neumann- This function computes the matrices obtained by evaluating the Neumann contribution of Neumann edges.

NeuNumb- This function assembles or includes the Neumann contribution of Neumann edges into the load vector.

Dirichlet- This evaluates functions defined on Dirichlet edges using nodes on these edges.

ReduceMatrix- Here we delete those rows/columns of Dirichlet nodes both on the load and stiffness matrices.

Writing- This functions returns a copy (as a text file) of the corrected stiffness matrix and load vector which are stored in the machine.

Soln - Returns the approximate solution u_h.

Recons - Reconstitute the vector of approximate solutions.

L2-Norm - Computes $\|u - u_h\|_{L_2}$.

H1-Norm - Computes $\|u - u_h\|_{H_1}$.

4.2 Model Problems

We consider in this section some model problems to demonstrate the robustness of the software developed. The first and second examples are mixed boundary value problems for the Poisson, Modified Helmholtz and Helmholtz equations on two different domains.

Here the exact solution is known and is regular. The third example is the mixed boundary value problem for the Helmholtz equation on an L-shaped domain. Here the exact solution and stress intensity factor are known, that is, our solution is singular.

On each domain considered, uniform refinement is done. That is, starting from an initial triangulation $\mathcal{T}_{h_1}$, finer triangulations are obtained by successively dividing each triangle into four smaller congruent ones.

In each table of results presented, we have the following;

- The parameter h represents the step size and is reduced by 2 from one refinement to the other.
- The number of nodes on each refinement represents the sizes of the matrices, that is, the stiffness matrix is of dimension (number of nodes $\times$ number of nodes), the load vector (number of nodes $\times$ 1) and the solution u_h, (number of nodes $\times$ 1).
- The error estimates $\|u - u_h\|$ are computed using the continuous L_2- norm and H^1- norm.
- The rate of convergence α is computed using (3.16).

Example 4.1. *Consider Example 3.1 given in Chapter 3 for $\lambda = 0$ and $\lambda = 0.5$. For this numerical experiment, the initial triangulation $\mathcal{T}_{h_1}$ and the succeeding ones $\mathcal{T}_{h_2}$ and $\mathcal{T}_{h_3}$ are given in, (Figure 4.1).*

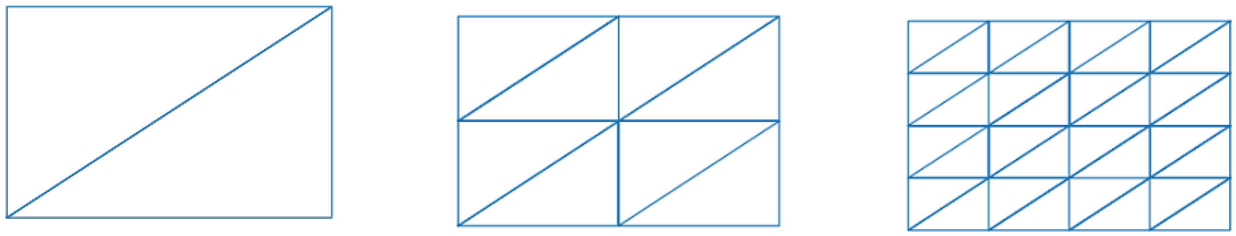

Figure 4.1: Ω: Initial triangulation $\mathcal{T}_{h_1}$, triangulation $\mathcal{T}_{h_2}$, triangulation $\mathcal{T}_{h_3}$.

Tables 1-2 give the error estimates $\|u - u_h\|$ in the L_2- norm and H^1- norm with their respective rates of convergence obtained using (3.16), for the Poisson and the Modified Helmholtz equations. According to Theorem 3.5, the expected convergence rates are $\alpha = 2$ in the $L_2(\Omega)$ norm and $\alpha = 1$ in the $H^1(\Omega)$ norm.

Table 1: The computed errors $\|u - u_h\|$ and the convergence rate α in the L_2- norm

h	# of nodes	$\|u-u_h\|_{L_2}$, $\lambda = 0$	α	$\|u-u_h\|_{L_2}$, $\lambda = 0.5$	α
2^{-2}	25	$1.6301977458\times10^{-1}$		$1.41531994806\times10^{-1}$	
2^{-3}	81	$4.446978646576\times10^{-2}$	1.87	$3.87222954023\times10^{-2}$	1.87
2^{-4}	289	$1.15293099657\times10^{-2}$	1.94	$9.9861634599\times10^{-3}$	1.96
2^{-5}	1089	$2.91191464899\times10^{-3}$	1.98	$2.52286772223\times10^{-3}$	1.98
2^{-6}	4225	$7.303709074084\times10^{-4}$	2.00	$6.32927861934\times10^{-2}$	2.00
2^{-7}	16441	$1.82785804501\times10^{-4}$	2.00	$1.58413357247\times10^{-4}$	2.00
Expected α			2.00		2.00

Table 2: The computed errors $\|u - u_h\|$ and the convergence rate α in the H^1- norm

h	# of nodes	$\|u-u_h\|_{H_1}$, $\lambda=0$	α	$\|u-u_h\|_{H_1}$, $\lambda=0.5$	α
2^{-2}	25	$8.90191422096\times10^{-1}$		$8.90972168478\times10^{-1}$	
2^{-3}	81	$4.72848234992\times10^{-1}$	0.91	4.729602043×10^{-1}	0.91
2^{-4}	289	$2.41268787097\times10^{-1}$	0.97	$2.41283407895\times10^{-1}$	0.97
2^{-5}	1089	$1.21395868334\times10^{-1}$	0.99	$1.21397719095\times10^{-1}$	0.99
2^{-6}	4225	$6.08118620829\times10^{-2}$	1.00	$6.08120942391\times10^{-2}$	1.00
2^{-7}	16441	$3.04224870229\times10^{-2}$	1.00	$3.04225160702\times10^{-2}$	1.00
Expected α			1.00		1.00

Example 4.2. *Let $\Omega \subset \mathbb{R}^2$ be an L-shaped domain and consider the following homogeneous mixed boundary value problem for the Helmholtz equation defined on Ω;*

$$
\begin{cases}
-\Delta u - 0.5u & = f \quad in \quad \Omega \\
u & = 0 \quad on \quad 0 \leq x \leq 1,\ y=0 \; and \, x=0,\ 0 \leq y \leq 1 \\
\frac{\partial u}{\partial n} & = 0 \quad on \quad -1 \leq x \leq 0,\ y=1 \\
\frac{\partial u}{\partial n} & = 0 \quad on \quad x=-1,\ -1 \leq x \leq 1 \\
\frac{\partial u}{\partial n} & = 0 \quad on \quad -1 \leq x \leq 1,\ y=-1 \\
\frac{\partial u}{\partial n} & = 0 \quad on \quad x=1,\ -1 \leq y \leq 0
\end{cases}
$$

where, $u = xy(y^2-1)^2(x^2-1)^2$ is the exact solution. The initial triangulation $\mathcal{T}_{h_1}$, triangulation $\mathcal{T}_{h_3}$ and triangulation $\mathcal{T}_{h_4}$ are given in Figure (4.2).

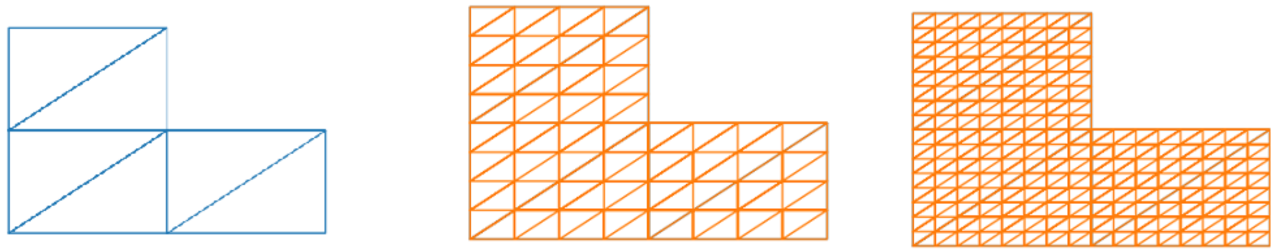

Figure 4.2: Ω: Initial triangulation $\mathcal{T}_{h_1}$, triangulation $\mathcal{T}_{h_3}$, triangulation $\mathcal{T}_{h_4}$.

Table 3 gives the error estimates $\|u - u_h\|$ and the rates of convergence in the L_2- norm and H^1- norm, where the expected rates are given in Theorem 3.5. The essence of this example is to show that eventhough the domain has a corner, the optimal rates of convergence are obtained because of the regularity of the solution.

Table 3: The computed errors $\|u-u_h\|_0$, $\|u-u_h\|_1$ and the rates of convergence α.

h	# of nodes	$\|u-u_h\|_{L_2}$	α	$\|u-u_h\|_{H_1}$	α
2^{-1}	21	$3.271300676534\times10^{-2}$		$2.012425327397\times10^{-1}$	
2^{-2}	65	$1.249896093557\times10^{-2}$	1.38	$1.299519874638\times10^{-1}$	0.63
2^{-3}	225	$3.577211495978\times10^{-3}$	1.80	$7.026190336525\times10^{-2}$	0.89
2^{-4}	833	$9.272155978833\times10^{-4}$	1.95	$3.586686919455\times10^{-2}$	0.97
2^{-5}	3201	$2.339241162902\times10^{-4}$	2.00	$1.802817265065\times10^{-2}$	1.00
2^{-6}	12545	$5.861177154968\times10^{-5}$	2.00	$9.026020728664\times10^{-3}$	1.00
Expected α			2.00		1.00

Following the analysis from (3.17), the following plot is obtained;

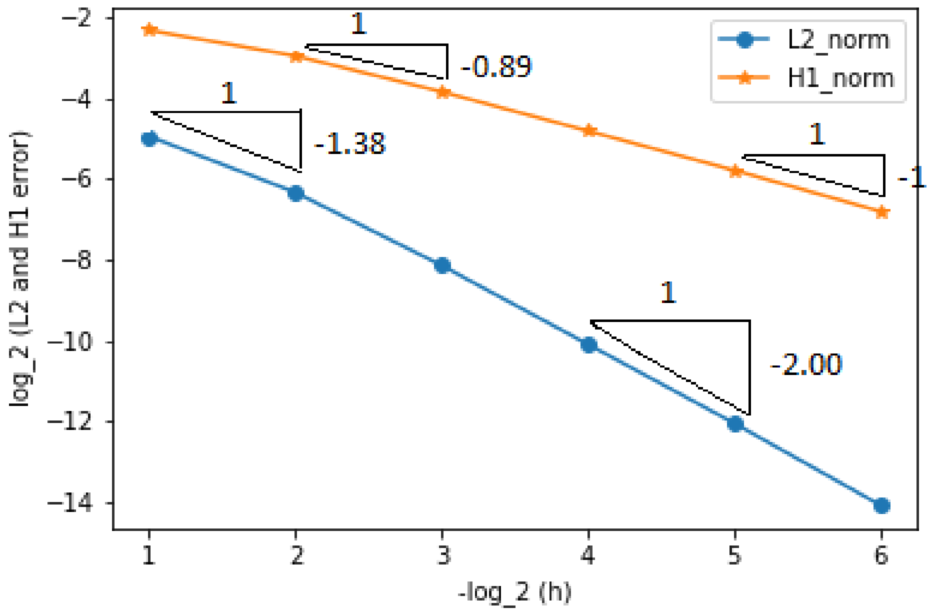

Figure 4.3: Plot of the estimate $\log_2(\|u - u_h\|_{L_2}), \log_2(\|u - u_h\|_{H_1})$ against $-\log_2(h)$

The graph above shows that both the error estimates $\|u - u_h\|_{L_2}$ and $\|u - u_h\|_{H_1}$ decrease as the discretization parameter h decreases. On this graph, we observe that;

- Initially, the line is not straight meaning that the rate of convergence is not yet constant as seen in table 3.
- Eventually when the rate becomes constant, the line straightens out and from Table 3, this occurs when $\alpha = 2$.
- The gradient α appears to be negative in the plot because we multiplied $log_2(h)$ on the $x-$axis by -1.

Now we consider the same domain but with a singularity in the solution and observe the order of convergence.

Example 4.3. *We consider the following mixed boundary value problem for the Helmholtz-equation defined on Ω, see Figure (4.2);*

$$\begin{cases} -\Delta u - 0.5u & = f \quad in \quad \Omega = \{(x,y) : -1 \le x \le 1,\ -1 \le y \le 1\} \\ u & = 0 \quad on \quad 0 \le x \le 1,\ y = 0 \ and \ x = 0,\ 0 \le y \le 1 \\ \frac{\partial u}{\partial n} & = h_1 \quad on \quad -1 \le x \le 0,\ y = 1 \\ \frac{\partial u}{\partial n} & = h_2 \quad on \quad x = -1,\ -1 \le x \le 1 \\ \frac{\partial u}{\partial n} & = h_3 \quad on \quad -1 \le x \le 0,\ y = -1 \\ \frac{\partial u}{\partial n} & = h_4 \quad on \quad 0 \le x \le 1,\ y = -1 \\ \frac{\partial u}{\partial n} & = h_5 \quad on \quad x = 1,\ -1 \le y \le 0 \end{cases}$$

where, the functions $f, h_1, h_2, h_3, h_4, h_5$ are chosen such that the exact solution is given by

$$u = xy(y^2-1)^2(x^2-1)^2+3r^{\frac{2}{3}}\sin\left(\tfrac{2}{3}\theta\right) \ with,\ r = (x^2+y^2)^{\frac{1}{2}} \ and\ \theta = \begin{cases} \arccos\left(\frac{y}{r}\right) \ for\, x \le 0 \\ 2\pi - \arccos\left(\frac{y}{r}\right) \ for\, x > 0 \end{cases}$$

Table 4 gives the errors of the finite element solution and the corresponding convergence rates in the $L_2(\Omega)$ and $H^1(\Omega)$ norms. According to Theorem 3.6, the expected rates are given to be $\alpha = \frac{4}{3}$ in the L_2- norm and $\alpha = \frac{1}{3}$ in the H^1- norm.

In Table 5, we present the errors of the approximations to the stress intensity factors which according to Theorem 3.6 are expected to be $\alpha = 4/3$.

Table 4: The computed errors $\|u-u_h\|_0$, $\|u-u_h\|_1$ and the rates of convergence α.

h	# of nodes	$\|u-u_h\|_{L_2}$	α	$\|u-u_h\|_{H_1}$	α
2^{-2}	21	$3.4297085788451\times10^{-1}$		$9.265520264938\times10^{-1}$	
2^{-3}	65	$1.4652555394635\times10^{-1}$	1.23	$6.007318285038\times10^{-1}$	0.63
2^{-4}	225	$5.9847281255911\times10^{-2}$	1.29	$3.819054822761\times10^{-1}$	0.65
2^{-5}	833	$2.4058864935723\times10^{-2}$	1.31	$2.4156482889413\times10^{-1}$	0.66
2^{-6}	3201	$9.605301112327\times10^{-3}$	1.32	$1.525305299635\times10^{-1}$	0.66
2^{-7}	12545	$3.8226006663825\times10^{-3}$	1.33	$9.622639813880\times10^{-2}$	0.66
Expected α			4/3		2/3

Table 5: The computed errors $|\gamma-\gamma_h|$ and the rates of convergence α.

h	# of nodes	γ_h	$\|\gamma-\gamma_h\|, \gamma=3$	α
2^{-2}	21	2.87930178957607	$1.2069821042392981\times10^{-1}$	
2^{-3}	65	2.88689600477259	$1.1310399522740999\times10^{-1}$	0.09
2^{-4}	225	2.95899144809207	$4.100855190793018\times10^{-2}$	1.46
2^{-5}	833	2.98295273984527	$1.7047260154730015\times10^{-2}$	1.27
2^{-6}	3201	2.99330325036770	$6.6967496323000475\times10^{-3}$	1.35
2^{-7}	12545	2.99747956295099	$2.5204370490099492\times10^{-3}$	1.41
Expected α				4/3

Remark 4.1. *Examples 4.2 and 4.3 corroborate the fact that the loss of standard finite element approximation accuracy for elliptic BVPs with corner singularities arises from the non-smoothness of the solution, see for example, [32].*

Applying the post processing algorithm described in [25] twice, we obtain the errors and convergence rates summarized in Tables 6 and 7. Here we expect the convergence rate of $\alpha = 2$ in the L_2- norm for $\|u-u_h\|$, $|\gamma-\gamma_h|$ and $\alpha = 1$ in H^1- norm for $\|u-u_h\|$, according to Theorem 3.7.

Table 6: The computed errors $\|u-u_h\|_0$ and $\|u-u_h\|_1$ after two post processing.

h	# of nodes	$\|u-u_h\|_{L_2}$	α	$\|u-u_h\|_{H_1}$	α
2^{-2}	21	$1.21524822995\times10^{-1}$		$9.8849431212876\times10^{-1}$	
2^{-3}	65	$3.71069786472\times10^{-2}$	1.71	$6.373602645971\times10^{-1}$	0.63
2^{-4}	225	$1.15851661901\times10^{-2}$	1.68	$4.0459830884\times10^{-1}$	0.66
2^{-5}	833	$3.60040229092\times10^{-3}$	1.68	$2.557808326775\times10^{-1}$	0.66
2^{-6}	3201	$1.12105173389\times10^{-3}$	1.68	$1.6145966980994\times10^{-1}$	0.66
Expected α			2.00		1.00

Table 7: The computed rates $|\gamma-\gamma_h|$ after two post processing

h	# of nodes	γ_h	$\|\gamma-\gamma_h\|, \gamma = 3$	α
2^{-2}	21	2.95340664898972	$4.659335101028006\times10^{-2}$	
2^{-3}	65	2.97982913930834	$2.0170860691659964\times10^{-2}$	1.21
2^{-4}	225	2.99542073671719	$4.579263282809887\times10^{-3}$	2.14
2^{-5}	833	2.99879821112039	$1.2017888796100884\times10^{-3}$	1.93
2^{-6}	3201	2.99968882747583	$3.111725241700114\times10^{-4}$	1.95
2^{-7}	12545	2.99992553096329	$7.446903671004534\times10^{-5}$	2.06
Expected α				2.00

4.3 Conclusions and Ways forward

In this thesis, the finite element method was applied for the computation of the solutions of the mixed-boundary value problem for the Poisson and Helmholtz-type equations in polygonal domains. The following were observed;

1. The mixed boundary value problems for the Poisson and the Modified Helmholtz equations with a smooth solution were considered. The net result was that the approximate solution converges to the exact solution as the step size $h \to 0$ with optimal rate of convergence.

2. Next the mixed boundary value problem for the Helmholtz equation with a singular solution was considered and the expected convergence rate was obtained. The observation here was that the accuracy of the finite element method was significantly reduced, that is the rate of convergence was reduced.

3. In an attempt to obtain a better convergence rate of the approximated solution, the predictor corrector adaptive technique due to, [25] was applied. Even though the stress intensity factors appeared to be well approximated, the solution on the other hand does not.

4. As future perspectives, we want to apply the traditional graded mesh refinement procedure on our domain with a corner to have optimal convergence rates and also consider higher order P-finite element methods for the achievement of better results.

Bibliography

[1] Apel, T., Heinrich, B.:Mesh refinement and windowing near edges for some elliptic problem. *SIAM J. Numer. Anal.*, 31(3):695-708, (1994)

[2] Aziz, A., Babuška, I.: *The Mathematical Foundations of the Finite Element Method with Applications to Partial Differential Equations*, Academic Press, Inc, New York, (1972)

[3] Babuška, I., Suri, M.: The h-p version of the finite element method with quasiuniform meshes, *RAIRO - Modélisation mathématique et analyse numérique*, 21(2):199-238, (1987)

[4] Bandar, A.: *The Method of Fundamental Solutions for Helmholtz- type Problems*, University of Leeds, (2013)

[5] Blum, H.: Numerical treatment of corner and crack singularities. In Stein, E., Wendland, W.L (eds) Finite element and boundary element techniques from mathenatical and engineering point of view, *CISM*, 301:172-212, Springer, (1998) .

[6] Boyce, W., Diprima, R.: *Elementary differential equations and boundary value problems*, Seventh edition, John Wiley and Sons, Inc, New York, (2001).

[7] Brezis, H.: *Analyse Fonctionnelle*,Théorie et applications, 2^e tirage, Masson, (1983).

[8] Burden, R., Faires, D.: *Numerical Analysis*, Ninth edition, Cengage Learning, Australia, (2010).

[9] Ciarlet, P.: *The Finite Element Method for Elliptic Problems*, Society for Industrial and Applied Mathematics (SIAM), Philadelphia, (2002)

[10] Ciarlet, J., Jung, B., Kaddouri, S., Labrunie, S., Zou, J.: The Fourier singular complement method for the Poisson problem. Part I: prismatic domains,*Numer. Math.* Springer-Verlag, (2005).

[11] Ciarlet, P., Lions, J.: *Handbook of Numerical Analysis, Finite Element Methods (Part 1)*, Elsevier Science B.V, North-Holland,(1991).

[12] Dauge, M.: *Elliptic Boundary Value Problems on Corner Domains*, Lecture Notes in Mathematics, No. 1341, Springer-Verlag, (1998).

[13] Debnath, L., Mikusiński, P.: *Introduction to Hilbert Spaces with Applications*, Academic Press, San Diego, (1990).

[14] Duchateau, P., Zachmann, D.:*Schaum's outline of the theory and problems of partial differential equations*, McGraw-Hill Book Company, New York, (1998).

[15] Evans, C.: *Partial Differential Equations*, American Mathematics Society, Berkely, (1997).

[16] Grisvard, P.: *Elliptic Problems in Nonsmooth Domains*, Pitman advanced publishing program, Boston-London, (1985).

[17] Grisvard, P.: *Singularities in Boundary Value Problems*, Springer-Verlag, (1992)

[18] Grossmann, C., Roos, H-G.: *Numerical treatment of partial differential equations*, Springer-Verlag, (2007)

[19] Gumerov, N., Duraiswami R.: *Fast multipole methods for the Helmholtz equation in three dimensions*, Elsevier Inc, San Diego, (2004)

[20] Jürgen, J.: *Partial Differential Equations*, Springer-Verlag, Inc, (2002)

[21] Křížek, M., Neittaanmäki, P.: *Finite Element Approximation of Variational Problems and Applications*, Longman Group UK Limited, New York, (1990)

[22] Lubuma, J., Nicaise, S.: Finite element method for elliptic problems with edge singularities, *Journal of Computational and Applied Mathematics*, 106:145-168, Elsevier, (1998)

[23] Marin, L., Lesnic, D., Mantič, V.: Treatment of singularities in Helmholtz-type equations using the boundary element method,*Journal of sound and vibration*, 278:39-62, Elsevier,(2004)

[24] Nakhle, H.: *Partial Differential Equations with Fourier Series and Boundary Value problems*, Second Edition, Pearson Education, Inc, London-Australia, (2005)

[25] Nkemzi, B., Jung, M.: A Postprocessing finite element strategy for Poisson's equation in polygonal domains: Computing the stress intensity factors, Apel T., Steinbach O. (Eds): Advanced finite element methods and applications.,*LNACM* 66:153-173,(2013)

[26] Rossum, G.: *Python reference manual*, CWI(Centre for Mathematics and Computer Science) Amsterdam, The Netherlands, The Netherlands, (1995).

[27] Schwab, C.: *p-and hp- Finite Element Methods. Theory and Applications in Solid and Fluid Mechanics*, Numerical Mathematics and Scientific Computation, Oxford University Press, (1998)

[28] Šolin, P.: *Partial Differential Equations and the Finite Element Method*, A John Wiley and Sons, Inc, New Jersey, (2006).

[29] Wamba, N.: Python Software, *https://drive.google.com/drive/folders /0B1Gc7rjHeFiQX0E4cVhSbmlGTUU?usp=sharing*, (2017)

[30] Wen, C., Zhang, J., Fu, Z.: Singular boundary method for modified Helmholtz equations, *Engineering Analysis with Boundary Elements*, 44:112-119, Elsevier Ltd, (2014)

[31] Wloka,J.: *Partial differential equations*, Cambridge University Press, Cambridge-London, (1987)

[32] Zhiqiang, C., Seokchan, K., Gyungsoo, W.: A finite element method using singular functions for the Poisson equation: crack singularities, *Numer. Linear Algebra Appl.*, 9:445-455,(2002)

[33] Zienkiewicz, O., Taylor,R., Zhu, J.: *Finite Element Method, Its Basis and Fundamentals* Sixth edition, Elsevier, Amsterdam-Boston, (2005).

Appendix

This part contains a sample of the code developed;

```
#Entering the polygonal domain. i.e we move from the individual

triangles to enter the entire domain.def InputPoly():

Results=input('Enter the path to the file containing the nodes

of triangles\n');Sheet=open(Results+'.txt','r')

z=[];Px=[];Py=[];D=[];N=[];B=[]readFile=open(Results+'.txt','r')

sepFile=readFile.read().split('\n');sepFile.remove('')

readFile.close();for plotFair in sepFile:

xa=plotFair.split(' ');for xb in xa:xc=xb.split(' ');z.append((xc[0]))

p=int(((len(z))/3));for n in range(0,p):

Px.append(float(z[3*n]));Py.append(float(z[3*n+1]))

B.append([float(z[3*n]),float(z[3*n+1]),(z[3*n+2])]);if (z[3*n+2])=='D':

D.append([(float(z[3*n])),(float(z[3*n+1]))])

for a in D:if D.count(a) > 1:D.remove(a)

elif (z[3*n+2])=='N':N.append([(float(z[3*n])),(float(z[3*n+1]))])

for b in N:if N.count(b) > 1:N.remove(b);for ap in B:if B.count(ap)>1:

B.remove(ap);Px.append(Px[0]);Py.append(Py[0]);x=[];y=[];s=[]

m=int(input('Enter the number of refinements desired please. '))

lamda=float(input('Enter the value of the constant lamda. '))

f1=input('Enter the source term please\nf(x,y)= ')

U=input('Please enter the true solution\n U(x,y)=')
```

```
plt.plot(Px,Py);plt.show()
while (Px!=[] and Py!=[]):x1=float(Px[0]);Px.remove(Px[0])
y1=float(Py[0]);Py.remove(Py[0]);x.append(x1);y.append(y1)
if len(x)==len(y)==3:s.append([x,y]);x=[];y=[]
return(Px,Py,s,m,lamda,f1,D,N,B,U);Px,Py,s,m,lamda,f1,D,N,B,U=InputPoly()
def AllEdges():
Results = input('Enter the path to the file containing the boundary edges
and functions. \n');Sheet = open(Results + '.txt', 'r')
z = [] ; Aedge=[];readFile = open(Results + '.txt', 'r')
sepFile = readFile.read().split('\n');sepFile.remove('');readFile.close()
for plotFair in sepFile:xa = plotFair.split(' ')for xb in xa:
xc = xb.split(' ');z.append((xc[0]));p=int((len(z)/5))
for n in range (0,p):
Aedge.append([[float(z[5*n]),float(z[5*n+1])],[float(z[5*n+2])
float (z[5*n+3])],(z[5*n+4])]);return Aedge;Aedge=AllEdges()
#Collecting all boundary edges.
def Edges(s):
E1=[];E=[];for e in s:for i in range(0,2):for j in range (i+1,3):
xn=[e[0][i],e[1][i]] ; yn=[e[0][j],e[1][j]] ; E1.append([xn,yn])
for plus in E1:if E1.count(plus)==1:E.append(plus);return E;E=Edges(s)
#Refinement.
def Ref( s,m):p=0;v=[];Mx=[];My=[];while p<m:Init1=[0];Init2=[0]
for a in s:for j in range (0,2):for k in range (j+1,3):
```

```
x2=(a[0][k]+a[0][j])/2;y2=(a[1][k]+a[1][j])/2;Mx.append(x2);My.append(y2)
Mx=[Mx[0],Mx[2],Mx[1]];My=[My[0],My[2],My[1]]
s1=[a[0][0],Mx[0],Mx[2]],[a[1][0],My[0],My[2]]
s2=[Mx[0], Mx[1],Mx[2]],[My[0],My[1],My[2]]
s3=[Mx[0],a[0][1],Mx[1]],[My[0],a[1][1],My[1]]
s4=[Mx[2],Mx[1],a[0][2]],[My[2],My[1],a[1][2]];si=[s1,s2,s3,s4]
Mx=[];My=[]:Vec1=Init1+s1[0]+s2[0]+s3[0]+s4[0]
Vec2=Init2+s1[1]+s2[1]+s3[1]+s4[1];Init1=Vec1;Init2=Vec2
for b in si:v.append(b);si=[];Vec1.remove(0);Vec2.remove(0)
p+=1;s=v;v=[];Vec1.append(Vec1[0])
Vec2.append(Vec2[0]);return (s,Vec1,Vec2);(s,Vec1,Vec2)=Ref( s,m)
#Collecting all nodes in the domain, including boundary nodes and
boundary coordinates of each node.
def Node(s):
Nodes=[] ; All=[] ; BCoor=[] ; BNode=[];for o in s:
if ([o[0][0], o[1][0]]) not in Nodes:Nodes.append([o[0][0], o[1][0]])
if ([o[0][1], o[1][1]]) not in Nodes:Nodes.append([o[0][1], o[1][1]])
if ([o[0][2], o[1][2]]) not in Nodes:Nodes.append([o[0][2], o[1][2]])
All.append([o[0][0], o[1][0]]);All.append([o[0][1], o[1][1]])
All.append([o[0][2], o[1][2]]);for f1 in Nodes:if All.count(f1) < 6:
BNode.append(Nodes.index(f1));for f2 in BNode:BCoor.append(Nodes[f2])
return Nodes, All, BNode, BCoor;Nodes,All,BNode,BCoor=Node(s)#Classifying
boundary nodes in the boundary they belong.
```

```
def Boundary(D,N,De,BCoor):

for bcoor in BCoor:for de in De:

if (de[0][0]<= bcoor[0]<= de[1][0])and(de[0][1]<= bcoor[1] <= de[1][1]):

D.append(bcoor);for a in D:if D.count(a)>1:D.remove(a);for nt in BCoor:

if nt not in D:N.append(nt);for b in N:if N.count(b)>1:N.remove(b)

return D,N

D,N= Boundary(D,N,De,BCoor)

def NeumannE(s,D1,N1):

Ne = [];for o in s:f1=[o[0][0],o[1][0]]f2=[o[0][1],o[1][1]]

f3=[o[0][2],o[1][2]];if (f3 in N1 and f2 in N1) or (f2 in N1 and f3 in N1)

(f3 in D1 and f2 in N1) or (f2 in D1 and f3 in N1):if f3[0]<=f2[0]

f3[1]<=f2[1]:Ne.append([f3,f2]);elif f2[0]<=f3[0] and f2[1]<=f3[1]:

Ne.append([f2, f3]);if (f3 in N1 and f1 in N1) or (f1 in N1 and f3 in N1)

or (f3 in D1 and f1 in N1) or (f1 in D1 and f3 in N1):

if f3[0]<=f1[0] and f3[1]<=f1[1]:Ne.append([f3,f1])

elif f1[0]<=f3[0] and f1[1]<=f3[1]:Ne.append([f1,f3])

if (f2 in N1 and f1 in N1) or (f1 in N1 and f2 in N1)or

(f2 in D1 and f1 in N1) or (f1 in D1 and f2 in N1):

if f1[0]<=f2[0] and f1[1]<=f2[1]:Ne.append([f1, f2])

elif f2[0]<=f1[0] and f2[1]<=f1[1]:Ne.append([f2, f1]);for w in Ne:

if Ne.count(w)>1:Ne[:]=(value for value in Ne if value!=w);Ne2=Ne

return Ne2

Ne2=NeumannE(s,D1,N1)
```

```
#Collecting global node numbering for each triangle in the domain

NNum= vector containing global nodes numbering of each triangle.
```